Coastal wetlands mitigate storm flooding and associated costs in estuaries

Fairchild, Tom P.; Bennett, William G.; Day, Brett; Skov, Martin; Moller, Iris; Beaumont, Nicola; Karunarathna, Harshinie; Griffin, John N.

Environmental Research Letters

DOI:
10.1088/1748-9326/ac0c45

Published: 07/07/2021

Peer reviewed version

Coastal wetlands mitigate storm flooding and associated costs in estuaries

Tom P. Fairchild[1]*, William G. Bennett[1], Greg Smith[2], Brett Day[3], Martin W Skov[4], Iris Möller[5], Nicola Beaumont[6], Harshinie Karunarathna[1], John N. Griffin[1]

[1] Faculty of Science and Engineering, Swansea University, Swansea SA2 8PP, UK

[2]CSIRO Land and Water, Hobart, Tasmania, 7001, Australia

[3]LEEP, University of Exeter, Exeter EX4 4ST, UK

[4]School of Ocean Sciences, Bangor University, LL59 5EG, UK

[5]Trinity College Dublin, D02 PN40, Ireland

[6]Plymouth Marine Laboratory, PL1 3DH, UK

Abstract

As storm-driven coastal flooding increases under climate change, wetlands such as saltmarshes are held as a nature-based solution. Yet evidence supporting wetlands' storm protection role in estuaries - where both waves and upstream surge drive coastal flooding - remains scarce. Here we address this gap using numerical hydrodynamic models within eight contextually diverse estuaries, simulating storms of varying intensity and coupling flood predictions to damage valuation. Saltmarshes reduced flooding across all studied estuaries and particularly for the largest – 100-year – storms, for which they mitigated average flood extents by 35% and damages by 37% ($8.4M). Across all storm scenarios, wetlands delivered mean annual damage savings of $2.7M per estuary, exceeding annualised values of better studied wetland services such as carbon storage. Spatial decomposition of processes revealed flood mitigation arose from both localised wave attenuation and estuary-scale surge attenuation, with the latter process dominating: mean flood reductions were 17% in the sheltered top third of estuaries, compared to 8% near wave-exposed estuary mouths. Saltmarshes therefore play a generalised role in mitigating storm flooding and associated costs in estuaries via multi-scale processes. Ecosystem service modelling must integrate processes operating across scales or risk grossly underestimating the value of nature-based solutions to the growing threat of storm-driven coastal flooding.

Keywords: Saltmarsh; Storm Surge Attenuation; Wave Attenuation; Flood Mitigation; Nature-based Coastal Protection; Coastal Storms

Introduction

Coastal communities are increasingly vulnerable to flooding[1–4] owing to on-going development in flood risk areas[5–7] and anthropogenic climate change leading to sea level rise and intensifying storms[8–11]. Large storms can raise coastal water levels by more than 5m above astronomic tidal levels[12], causing extensive coastal flooding[13–15], as exemplified by the devastating impacts of Hurricane Harvey in the USA and Caribbean[14,16] in 2017, Super Typhoon Haiyan in the Philippines in 2013[17], and the 2013-14 winter storms in the UK and Europe[18,19]. Current predictions suggest that by 2100, annual coastal flooding will directly affect up to 5% of the world's population and cost up to 20% of global gross domestic product per year[4,20]. Although flood risks have traditionally been managed by building seawalls and other hardened defence structures[21–23], the emerging paradigm of nature-based coastal protection holds that resilient, wave- and surge-absorbing wetlands such as saltmarshes and mangroves should be integrated into coastal planning and management to more sustainably and effectively mitigate flood risk and impacts[24–27]. However, quantifying and valuing the contribution of ecosystems to flood mitigation is fraught with uncertainty due to multi-scale interactions between ecological features and hydrodynamic processes[28–31]. In particular, understanding how ecosystems influence flood risk in estuaries – physically complex environments of high socioeconomic significance – remains a pressing and challenging question.

Unlocking our understanding of nature-based coastal protection within estuaries is vital because these environments are particularly at risk of increased storm-driven surge and wave flooding; estuaries often have low-lying adjacent land[7,32–35], act as an interface between flood waters from coastal surge and riverine flooding[29,36,37], and form natural tidal and storm funnels which magnify and transfer surge effects up-stream[36,38], threatening inland human settlements and infrastructure[39,40]. Yet despite the enhanced flooding risk in estuaries, natural coastal protection features - such as extensive saltmarshes which typify many estuaries worldwide - can moderate the effects of coastal storms on flooding[25,30] and potentially offer significant

nature based coastal protection services[26,41]. However, there is a growing urgency to understand how estuarine marshes contribute to coastal flood mitigation, as the combined effects of human-induced pollution, increasing urbanisation and climate change are driving net global losses of these protective coastal wetlands[42–45], and could undermine their ability to perform storm defence functions[46].

Previous studies on open, exposed sections of coastline[e.g.47–49] have shown that saltmarsh vegetation increases hydrodynamic drag[31,50,51], locally attenuating waves[47,48] and surges[49,52] travelling over marshes towards the shoreline. Yet, in estuaries, upstream surge mitigation – whereby marshes cumulatively attenuate surge over large distances along confined estuary channels – is also likely to act in unison with local processes, mitigating impacts in vulnerable upstream regions[53–55]. Despite evidence of both localised and upstream, estuary-scale, dampening of waves and surge in isolation, there remains a lack of knowledge on how these multi-scale processes interact to holistically reduce flood risk and impacts throughout estuaries (Supplementary Table S1) (Figure 1). Accordingly, the contributions of saltmarshes to storm flood mitigation may be grossly underestimated and economically undervalued[56,57].

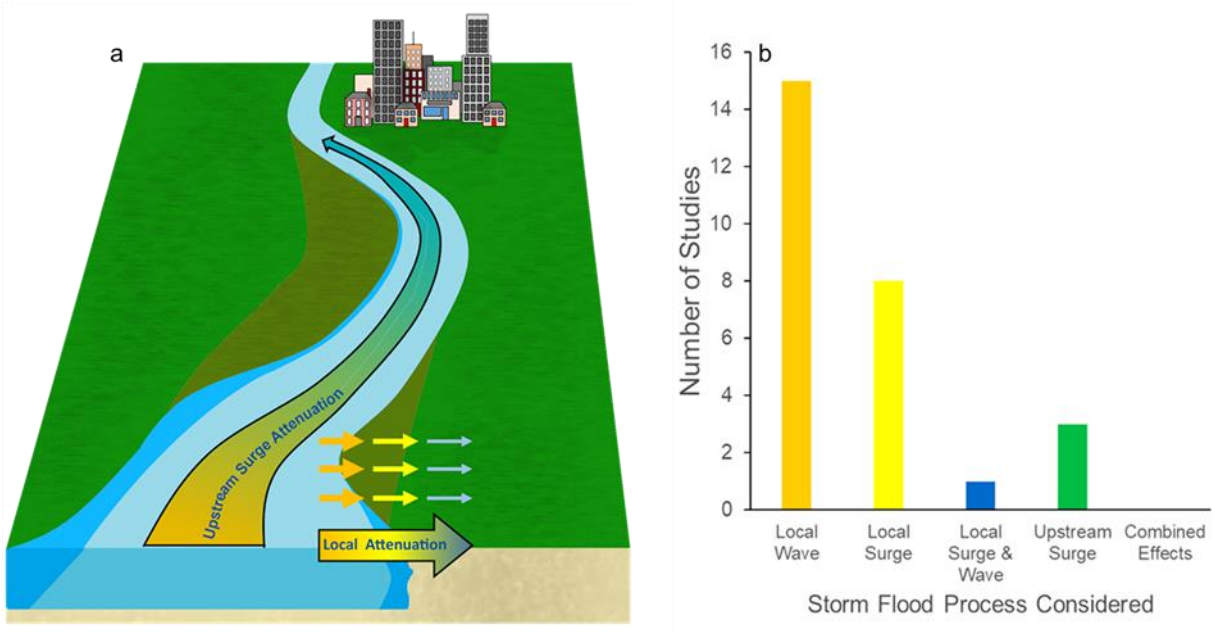

Figure 1: The undervalued role of localised and estuary-scale storm attenuation processes for enhancing storm flood mitigation in estuaries. **a**) Marshes provide localised wave and surge attenuation, and estuary-scale cumulative drag as surge moves upstream in estuaries, reducing upstream surge risk. Warmer colours represent higher surge and wave heights, and cooler colours represent lower wave and surge heights. **b**) The number of existing studies examining the role of vegetation in reducing

flood risk through processes operating at different scales (Supplementary Table S1). Note the absence of previous studies investigating combined effects (local surge/wave *and* upstream surge).

Here we address the current uncertainty in the role of coastal wetlands in flood mitigation within estuaries by integrating both localised attenuation and estuary-scale processes. Specifically, we investigated the role of marsh vegetation in reducing flooding and flood impacts – at both local and estuary scales – across a range of estuaries which varied in size, morphology, tidal properties, marsh characteristics, and storm exposures, spanning a wide cross-section of comparable global estuary morphologies and environmental contexts[34,58–60]. We used high-resolution hydrodynamic simulations across eight estuaries, examining how vegetation state and storm intensity affects the degree of protection - both from flooding and resulting economic damages - offered by marshes. Our results demonstrate that saltmarshes play a substantial role in mitigating the effects of storm-driven flooding in estuaries through a combination of localised wave attenuation near estuary mouths, and whole-estuary scale reductions in upstream surge.

Results

Estuary-scale flood mitigation

We first examined the overall role of vegetated saltmarshes in mitigating coastal flooding at the estuary-scale across storm scenarios. Vegetated saltmarshes reduced both the extent and depth of flooding for all estuaries and storm scenarios considered within our study. Ungrazed, vegetated marshes reduced mean terrestrial flood extent by 34.5% (SD±24.1), and grazed marshes by 29.1% (SD±20.6), compared with unvegetated mudflats (Figure 2a, Supplementary Table S2). While the mean relative contribution of marshes to flood reduction slightly decreased with increasing storm intensity (Supplementary Table S2, Figure 2a), variability between estuaries decreased markedly. Flood water levels were also considerably reduced by vegetated marshes (Figure 2b), with mean reductions across the storm scenarios of 43.6% (SD±23.9) for fully vegetated marshes, and 35.7% (SD±22. 3) for grazed marshes, compared to unvegetated scenarios. Within estuaries, the proportion of marshes, as well as the vegetation state (vegetated, grazed, unvegetated), played a crucial role in reducing

flooding, with estuaries that have a proportionally higher cover of vegetated saltmarsh mitigating both flooding extent and water depth (Figure 2d, Supplementary Table S3 & S4).

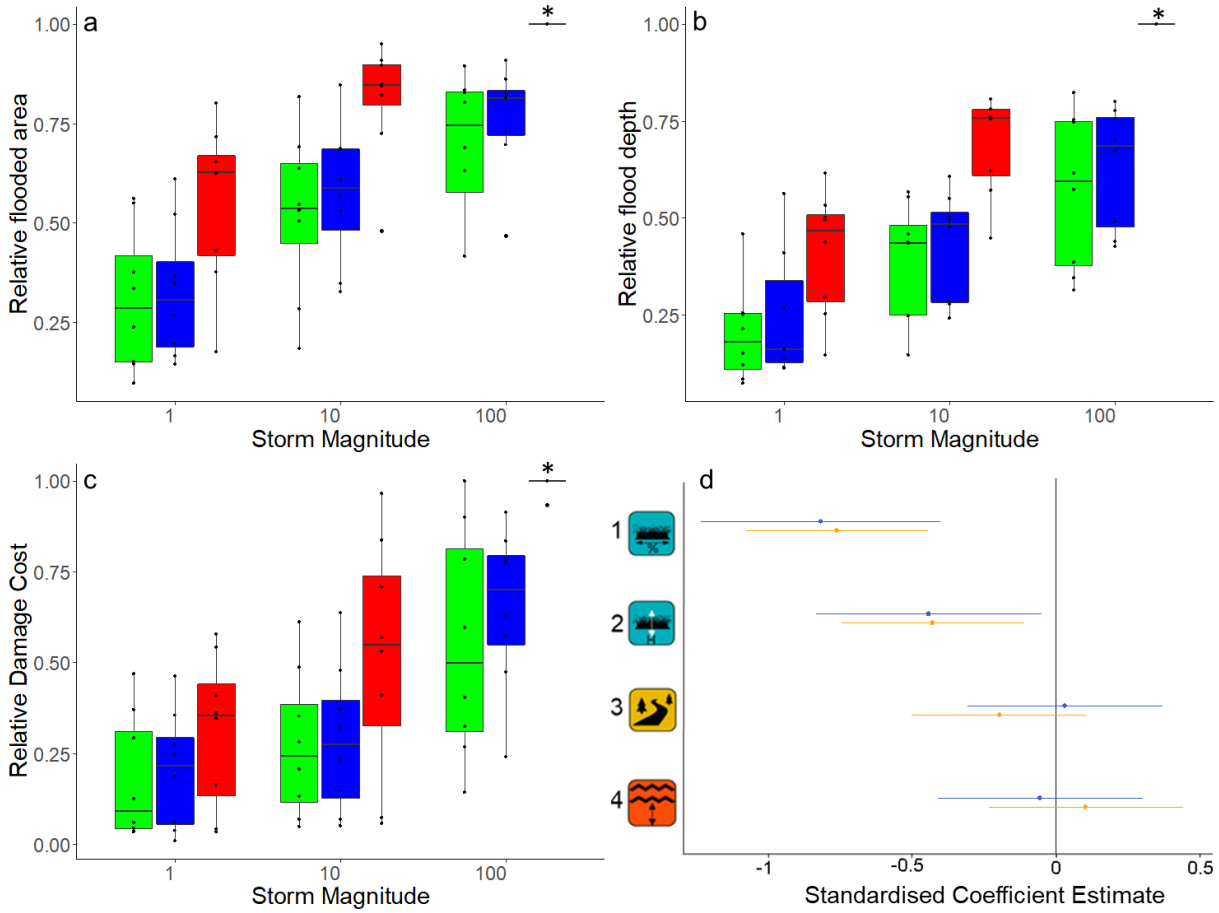

Figure 2: Vegetated saltmarshes mitigated flooding and economic costs across storm scenarios. The panels show relative flooded area (**a;** n=72), relative flood depth (**b;** n=72) and relative damage cost (**c;** n=72) across storm scenarios where marshes are vegetated (green), grazed (blue) or unvegetated (red). Bars with asterisks denote the unvegetated scenarios for the 1 in 100 year storms which were always proportionally the largest. Central boxplot line represents the mean, boxes the 25th-75th percentile, whiskers the minimum and maximum, and dots represent raw data points. **d**) Coefficient plot of drivers of estuary level flood mitigation for flood extents (orange) and flood depth (blue) by (top to bottom): Marsh area percentage (of total estuary area), Marsh vegetation height (grazed or ungrazed), Sinuosity of estuary channel and Estuary Tidal prism. Points represent estimates, and outer bars a 2-standard deviation CI (95%). Negative estimate values represent net benefits, i.e., flood mitigation.

Accompanying the reduction in flood extents and depths, vegetated marshes reduced the relative economic costs from damage to residential and commercial properties, infrastructure, and agricultural land, compared with the unvegetated scenarios across all storm events (Figure 2c, Table S5). However, unlike the depth and relative flood extents, vegetated marshes drove substantially greater savings in relative flood cost as storm magnitude increased. Under the 100-year return level storm events, where the potential for catastrophic

129 flooding was higher, vegetated marshes reduced flood water depth at the terrestrial boundary
130 leading to fewer banks and defences overtopping, mitigating resulting flooding and economic
131 costs. Notwithstanding the general economic savings observed across estuaries, vegetation
132 drove an increase in flood damage in a single estuary, where vegetation slowed the upstream
133 passage of surge (Supplementary Figure S1) during a large (100 year) storm, enhancing
134 localised flooding in particularly low-lying land near the estuary mouth.

135 Savings of damage costs driven by vegetation equated to an average saving per estuary of
136 37.1% ($8.4M, SE±$4.6M) for single 100-year return level storms, compared to 31.6% ($3.3M,
137 SE±$1.9M) and 20.5% ($1.36M, SE±$0.7M) for single 10-year and annual return-level storms
138 respectively (Supplementary Table S5). Across all storm scenarios, this equated to mean
139 annualised cost reduction of 37.8% ($2.7M, SE±$0.4M) per estuary (Supplementary Table
140 S6), and a mean flood protection value of $4772 (SE±$1285) per hectare, per year. Despite
141 inter-estuary differences in marsh value for flood mitigation, mean reductions in flooding cost
142 compared favourably to other valuable ecosystem services (Supplementary Table S7).

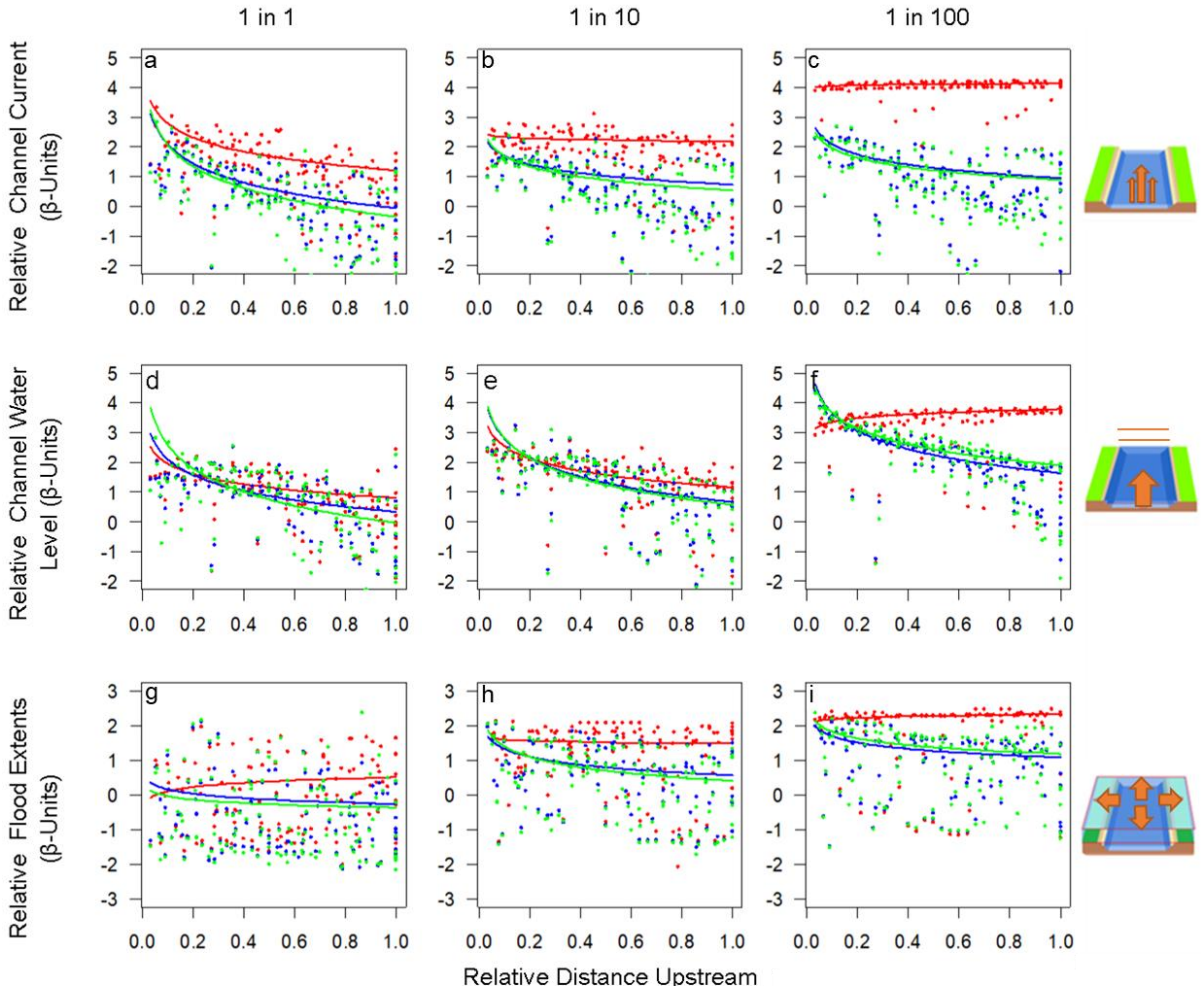

Figure 3: Vegetated saltmarshes reduced current velocities, water level and flood extents, particularly for large storms. Top: mean estuary section flood current relative to the maximum estuary section flood current by the proportional distance up-river for **a**) 1 in 1 year storm intensity (n=404), **b**) 1 in 10 year storm intensity (n=397) and **c**) 1 in 100 year storm intensity (n=404). Centre: mean estuary channel water level relative to the maximum observed, by the proportional distance up-river for **d**) 1 in 1 year storm intensity (n=404), **e**) 1 in 10 year storm intensity (n=397) and **f**) 1 in 100 year storm intensity(n=404). Bottom: Flooded area extents relative to the maximum observed, by the proportional distance up-river for **g)** 1 in 1 year storm intensity (n=404), **h**), 1 in 10 year storm intensity and (n=397) **i**) 1 in 100 year storm intensity (n=404). Points represent flood area, water level and velocity model estimates, given in beta-regression standardised values (*β-units*), and lines represent model fits for vegetated (green) grazed (blue) marshes, as well as where marshes were absent (red).

Upstream surge mitigation

To investigate the mechanisms underpinning marsh mitigation of coastal flooding, we first examined how marshes modify indicators of upstream storm surge propagation within sequential 1km estuary sections. Modelled differences in channel current and water levels between the vegetated and unvegetated scenarios showed a clear pattern of greater divergence with increasing distance upstream. Cumulative drag from fringing vegetation weakened upstream surge through net reductions of surge-driven flood currents (Figure 3a-c,

Figure 4c,d, Supplementary Table S8), limiting propagation of surge to inner-estuary areas. Accordingly, vegetated marshes also led to faster attenuation of storm-surge water levels with increasing proportional distance upstream (Figure 3d-f, Supplementary Table S9, illustrated in Figure 4a,b). At the same time vegetated marshes amplified surge level close to the estuary mouths, as surge was less able to dissipate by moving upstream. Both phenomena - water level suppression upstream and surge amplification towards the mouth - increased with storm intensity, indicating that the relative contribution of marshes to surge mitigation upstream increases with increasing storm magnitude. In line with the reduction in surge current and water levels, vegetated marshes ultimately more strongly reduced flooding with increasing distance upstream: vegetation drove mean reductions in flood extent by 16.7% in the inner estuary areas, compared to 8% in the outer-estuary areas for large storms (Figure 3g-i, Supplementary Table S10). Grazing of the marshes appeared to have very little effect on storm surge attenuation as indicated by both water level and currents.

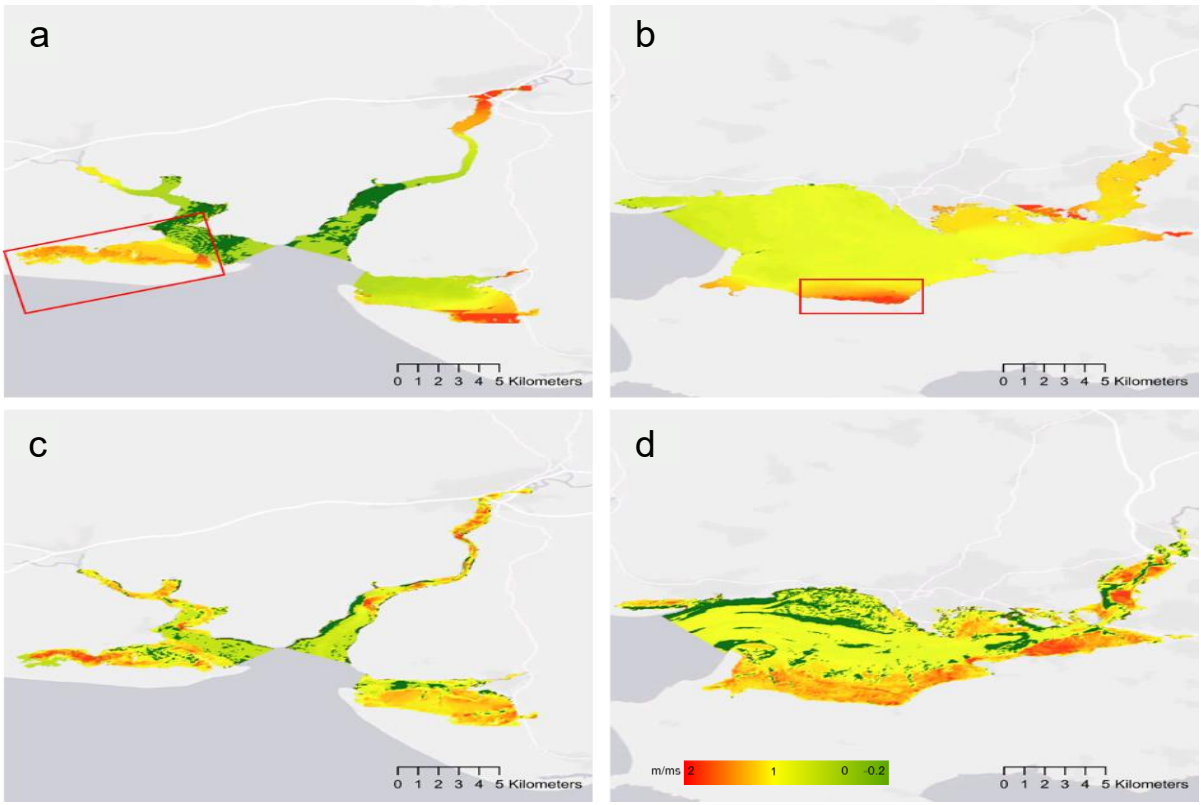

Figure 4: Vegetated saltmarsh reduced water level and flood current velocities in studied estuaries, illustrated with two examples from 1 in 100 year storms. Differences in water level (top) and flood current velocities (bottom) for vegetated marshes in the Three Rivers estuary complex (Taf, Towy, Gwendraeth; **a,c**) and Loughor Estuary (**b,d**) compared to where marsh vegetation is absent. Positive values indicate where vegetation reduced water level or current velocity, whereas negative values represent increases in water level or velocity. Red boxes over the water level figures (top) highlight localised flood events driven by wave overtopping, with water level differences represented in meters. For the currents (bottom), localised increases in current velocity in main channels when marsh vegetation is present are represented (dark green), while most of the estuary areas saw velocities slightly decrease (yellow), and over-marsh areas showed larger reductions, up to 1.8m/s (red).

We also noted that the effect of vegetation on surge propagation to up-stream areas responded to estuary size, with marsh vegetation reducing mean relative channel water levels at the limit of tidal intrusion more in smaller estuaries (Figure 5, Supplementary Table S11). These scale effects suggest that small estuaries benefit more from surge reduction due to the presence of marsh vegetation than larger estuaries. This effect was independent of the proportion of marsh area within estuaries, and effects on upstream surge water levels were observed for all storm scenarios.

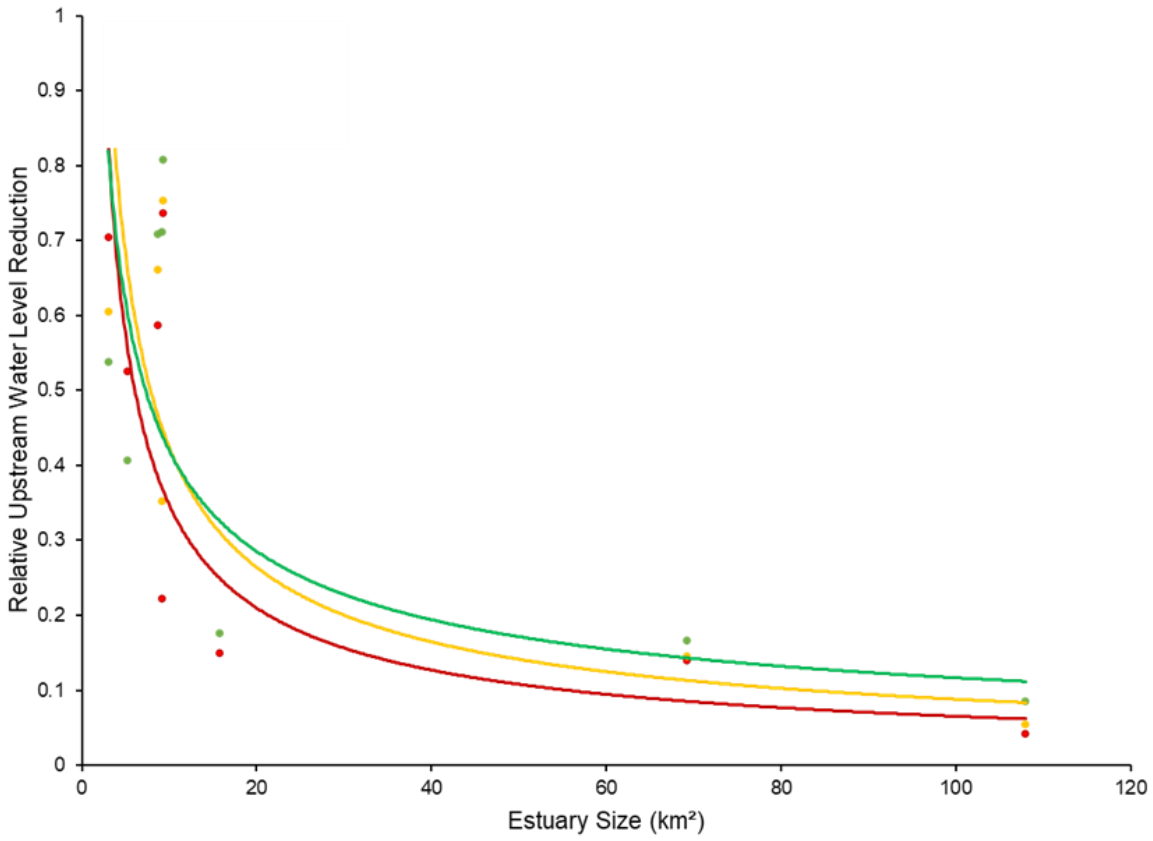

Figure 5: Upstream reduction in surge propagation by vegetated saltmarshes appear to become less important with estuary size, independently of marsh area extent. Proportional reductions in mean storm water levels between the fully vegetated and unvegetated scenarios compared with estuary size (km²) (n=24). Lines represent model fits for 1- (green points and line), 10- (yellow points and line) and 100-year (red points and line) storm events.

Wave and localised surge transformation

In addition to the estuary-scale surge attenuation, we observed vegetated marshes also drove localised decreases in flooding extent and depth, with effects particularly pronounced in wave-exposed outer-estuary areas (see Figure 4 for illustration) suggesting an important dual role of wave attenuation. To begin further investigating the mechanisms of storm wave attenuation in our study estuaries, we examined how saltmarshes influence wave heights in the estuary channel. Our focal metric was wave height relative to the maximum observed within an estuary sector to control for differences in absolute wave height across estuaries and with distance upstream (see *Methods*).

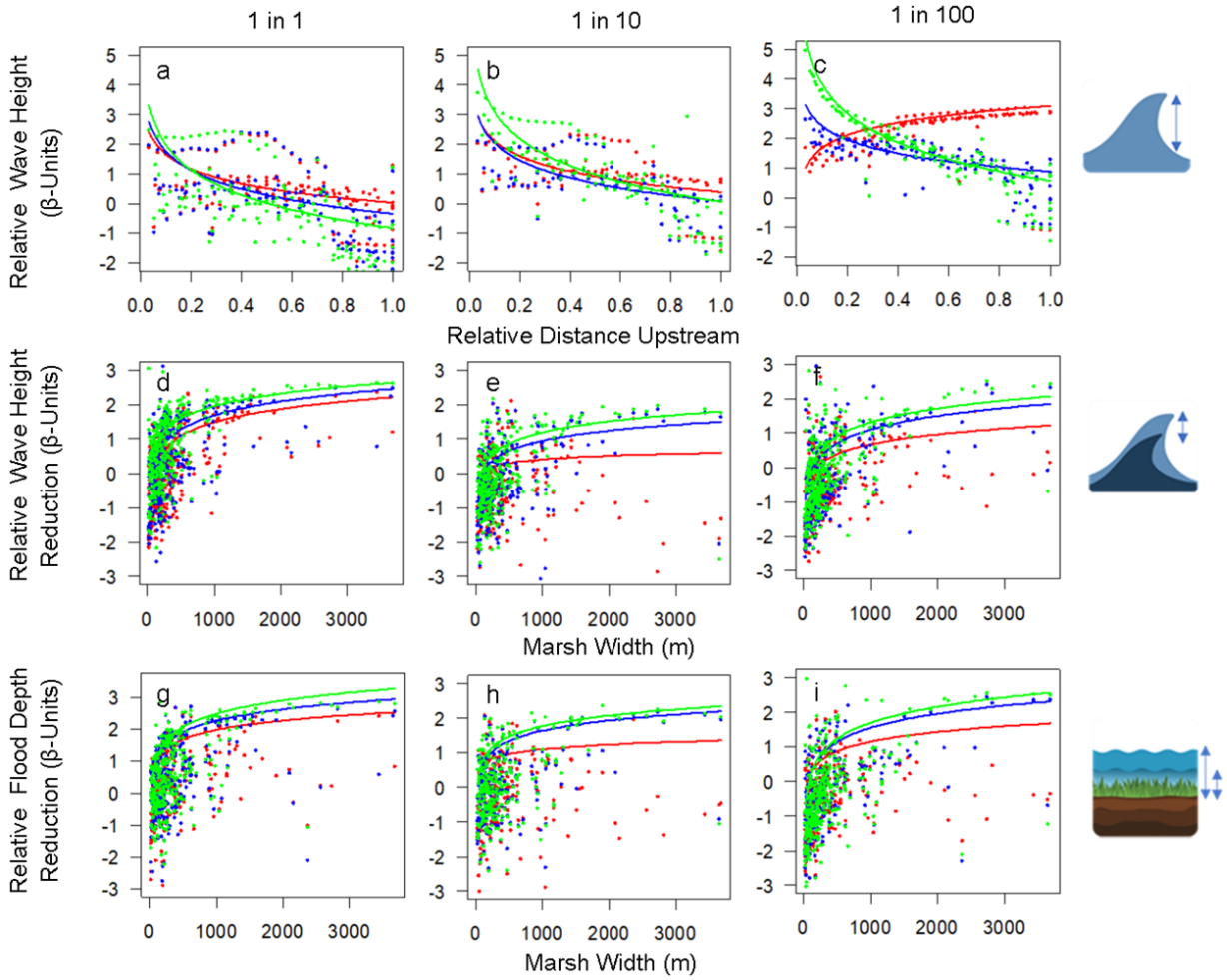

Figure 6: Vegetated saltmarshes reduced wave heights and flood depths at marsh edges, particularly for large storms. Top: Wave heights relative to the maximum observed, by the proportional distance up-river for **a**) 1 in 1 year storm intensity (n=404), **b**) 1 in 10 year storm intensity (n=397) and **c**) 1 in 100 year storm intensity (n=404). Centre: Relative wave reduction from marsh edge to terrestrial boundary by vegetation across transects for different marsh widths during **d**) 1 in 1 year storm intensity (n=997), **e**) 1 in 10 year storm intensity (n=836) and **f**) 1 in 100 year storm intensity (n=1022). Bottom: Relative flood depth reduction at the terrestrial boundary relative to the maximum observed depth, for different marsh widths during **g**) 1 in 1 year storm intensity (n=997), **h**) 1 in 10 year storm intensity (n=836) and **i**) 1 in 100 year storm intensity (n=1022). Points represent Area, Depth and Velocity partial estimates, given in beta-regression standardised values (β-units), and line represent model fits for vegetated (green) and grazed (blue) marshes, and where marsh vegetation is absent (red).

Differences in wave heights as a function of vegetation state increased with proportional up-stream distance and storm intensity, with the effect of vegetation far stronger and more consistent for the 1 in 100 year storm scenario than either 1 in 1 or 1 in 10 year scenarios (Figure 6a-c, Supplementary Table S12). These results indicate that, compared with unvegetated scenarios, vegetated saltmarsh reduced up-stream propagation of waves through estuary channels, particularly under the largest storms. However, vegetated marshes also tended to amplify wave heights in channels towards the estuary mouths for all storm scenarios, increasing water depth over shallow estuary mouth structures and in turn allowing

higher energy waves to propagate into estuaries[61,62]. Yet, at these outer-estuary locations, the aforementioned increases in surge height (Figure 3d-f), as well as these now described amplified wave heights, generally did not translate into increases in terrestrial flooding (Figure 3g-i). Instead, marsh vegetation offset increases in surge and wave height within estuary channels via localised transformation of waves and surge travelling landward over the marshes, ultimately decreasing flooding.

Indeed, examination of wave and surge transformation along transects perpendicular to the shoreline revealed vegetated marshes – particularly wide marshes characteristic of the lower-reaches of estuaries – reduced relative wave height and flood depth at the terrestrial boundary and these benefits increased with marsh width (Figure 6d-f). Smaller, narrower marshes also provided local flood reduction benefits through direct attenuation of landward wave and surge but these benefits were more variable, depending on the hydrodynamic and topographical context of their location. Unlike the estuary-scale effects of vegetation on water level and currents, grazing consistently and negatively impacted on marsh ability to attenuate incoming waves (Figure 6d-f) leading to greater flooding adjacent to the marshes, particularly for wide marshes. The relative impact of grazing on wave-attenuation appeared to be most pronounced for smaller storms but was also evident for the larger storms.

Discussion

The utility of nature-based coastal flood protection strategies has been extensively supported along open coastlines but remains uncertain within estuarine systems due to the complex, multiscale interactions at play in these socially and economically vital environments. Using high resolution modelling across a set of eight diverse estuaries we reveal the general importance of vegetated saltmarshes - regardless of grazing management - in mitigating flooding and associated economic costs across a range of storm scenarios. Crucially, while our models confirm the local scale wave attenuating effects of saltmarshes, they also reveal a far less quantified or appreciated effect of large-scale flood mitigation via surge attenuation, with benefits magnifying up-stream, under more extreme storm scenarios, and with greater

proportion of marsh area within an estuary. Furthermore, beneficial effects of marshes appear strongest within the smallest estuaries. Collectively, our results demonstrate that the role of marsh vegetation is more critical for reducing flood impacts - particularly in small estuaries - than previously assumed.

Our results show that local-scale surge and wave attenuation work together with larger-scale upstream surge attenuation to deliver substantial mitigation of coastal flooding, and subsequent flood damages, under a range of storm scenarios and estuary contexts. We found that, by attenuating waves and surge travelling perpendicular to the shoreline, marshes have the strongest localised dampening effects close to the estuary mouths where marsh widths and wave energy are highest, in-line with previous results from exposed coastlines[48,52,63]. However, larger, and more consistent flood extent and water level reductions were observed at wave-sheltered upstream locations. Observed strong and progressive divergence between vegetated and unvegetated scenarios with distance upstream clearly indicates that upstream flood reduction is driven by cumulative estuary-scale surge attenuation, suggesting that vulnerable up-stream human settlements rely heavily on downstream marshes in mitigating surge-driven flooding. Furthermore, the greatest reductions in localised wave attenuation occur across wide marshes, while the strongest large-scale surge attenuation occurs in estuaries with extensive marsh areas, indicating that greater relative marsh area has both local and large-scale flood mitigation benefits. Within estuaries, this interplay between the role of long-distance surge mitigation, and limited local wave and surge reduction in our study adds to previous work emphasising direct local wave- and surge- attenuation along exposed coastlines[e.g.53,64,65], to reveal the under-appreciated role of marshes within typically wave-sheltered small estuaries. Furthermore, within the size ranges of estuaries (3-108km^2) in our study, the role of marsh vegetation in attenuating upstream surge was stronger in the smallest estuaries, consistent with previous evidence of scale-dependence of surge mitigation along creeks[54], as well as theoretical work on the morphology and configuration of estuary channels[66–68], and is supported by smaller surge reductions observed in the much larger

Scheldt estuary[69](~370km²). The extension of the coastal protection paradigm to estuaries, and the suggestion these services may be even stronger in the smallest estuaries, is globally significant because small to medium sized estuaries are most common across many countries[34,58–60,70] while also being particularly vulnerable to amplification of surges driven by sea level rise[38,71].

Marsh mitigation of storm flooding has accompanying economic benefits, reducing flood damage costs by an average of 37% for large storms across the estuaries within our study. Savings from ungrazed and grazed marsh vegetation scaled exponentially with storm intensity, with the relative marsh-driven cost savings considerably higher than the 1-16% savings previously predicted for similar significant tropical storms along open coastlines dominated by extensive fringing or back-barrier marshes[41,57,72]. The estimated absolute flood damage savings within estuaries are similar to those previously estimated for hurricane-exposed US coastlines[73,74], and considerably greater than the value of other saltmarsh services such as carbon storage[75,76] or livestock grazing[77,78]. Indeed, in our study average flood mitigation from marshes - per hectare per year - was valued at between 22-75 times that of carbon storage, and 117 times that of grazing (Supplementary Table S7). Furthermore, these high relative flood mitigation service values were consistently observed across seven of the eight estuary case studies, despite inter-estuary variability. Accordingly, our new estimates serve as a tool to generate greater public and policy-maker recognition of the nature-based flood mitigation services in these deceptively sheltered environments, and substantially enhances the economic case for saltmarsh conservation and restoration. Even so, as our reported estimates relate exclusively to flood mitigation, they will underestimate the total value of marshes for coastal protection, including the role of vegetation in reducing shoreline erosion[79,80], and maintaining wave and surge attenuating raised marsh platforms[26]. In our study, flood-mitigation economic benefits of marshes can be considered general, with vegetation driven reductions in flood cost occurring in 7 of the 8 estuaries, but not universal: in one heavily modified estuary, extensive high-crested channelisation prevented flooding

upstream while vegetation enhanced surge water levels in downstream, densely populated areas, leading to a modest increase in flood damages when vegetation was present. Yet despite this inevitable context dependency, arising from interactions between physical, ecological and anthropogenic features, we find strong evidence for general patterns of marsh-driven reductions in economic costs from storm flood events.

Our results have important implications for marsh management for ecosystem services. Previous valuation and ecosystem service mapping approaches have considered the more direct effects of marshes on coastal protection – emphasising marshes in wave-exposed locations and fronting valuable infrastructure[56,56,81,82]. Clearly, it is vital that tools used for valuation of coastal protection services evolve to include the dominant process of long-distance surge mitigation, in addition to the better integrated direct contributions of marshes and other coastal systems to flood mitigation. Accordingly, marsh conservation and restoration must be treated at the whole estuary scale, with an understanding that marshes in highly wave-sheltered locations, or fronting areas with low flood vulnerability, may still be providing essential flood mitigation services further upstream. Our findings, from a diverse set of environmental and estuarine contexts, suggest that these estuary-scale effects are broadly applicable, although further studies may be needed to support our conclusions in less common estuary types which we did not examine in our study: particularly in large delta or coastal plain, or back-barrier estuaries where estuarine hydrodynamics may be different, and alter the contributions of marsh vegetation to flood mitigation. Importantly, our results suggest that marshes can be managed for multiple benefits, with grazing generally having only small influences on wave attenuation and surge mitigation – indicating that maintaining or enhancing marsh extent, rather than grazing pressure, should be a priority for flood mitigation management. Looking ahead, as climate change is predicted to bring increasing frequencies[3], and magnitudes[10,14,83] of large storms, with current 1 in 100 year storm water level events expected annually by 2100[84], our results indicate that appropriate valuation and effective

management of marshes is paramount to mitigate rising risks of flooding and its social and economic impacts.

In conclusion, our study demonstrates that coastal wetlands strongly reduce storm flooding and its economic consequences through both local and estuary-scale processes. Our research demonstrates that current valuation tools based on local-scale interactions oversimplify and underestimate contributions by coastal marshes to flood mitigation in estuaries where storm flooding threatens homes, industry, and infrastructure. Furthermore, we show that marshes mitigate flooding across a range of estuarine and environmental contexts, suggesting that our results will also apply to many other estuaries worldwide. Ecosystem service modelling and decision making in estuarine socio-ecological systems must now move towards integrating multi-scale processes or risk underestimating the value of wetlands and their conservation for protecting communities in the face of rising flood risk.

Methods

Site characteristics

To investigate the role of saltmarsh vegetation in reducing storm flood risk we examine eight case study estuaries along the coast of Wales, UK (Supplementary Figure S5) which explicitly differed in their size, morphology, marsh extents and exposure to storm events, reflecting the inherent morphological and environmental variability of estuaries[34,58–60,70,85]. The selected estuaries represented a broad range of characteristics to examine the generality of vegetation effects within estuaries: across large tidal range gradients (from mesotidal estuaries with ranges of ~3m, up to large macrotidal >10m ranges), wave exposure driven by wind fetch (<100km to >1000km), and estuary sizes (3km² to >100km²) and types. While not exhaustive, the environmental and topographical variation across our case-study estuaries broadly represent the properties of many common small-to medium sized estuaries which are described in the literature[59,60,86]. These differences, and differences in prevailing conditions, allowed us to explore the role marshes play irrespective of environmental context, and

investigate potential interactions between marsh vegetation and estuary characteristics in moderating flooding. The properties of each estuary are summarised in Table 1.

Table 1: Summary of the properties of estuaries used in this study.

	Estuary	Estuary Area	Estuary Tidal Prism (m^3)[a]	Tidal Range (m)[b]	Estuary Type[c]	Estuary Orientation[d]	Estuary Sinuosity[e]	Saltmarsh %[f]
1	**Neath**	3.00km^2	15,050,000	10.3	Ria	45°	1.264	30.3%
2	**Loughor**	69.25km^2	244,879,000	9.7	Coastal Plain	47°	1.506	31.6%
3	**Gwendraeth**	8.71km^2	14,874,000	8.9	Bar built	98°	1.288	69.0%
4	**Towy**	9.33km^2	23,378,000	8.9	Coastal Plain	9°	1.325	26.3%
5	**Taf**	9.20km^2	14,840,000	8.9	Coastal Plain	308°	1.444	36.5%
6	**Mawddach**	5.22km^2	10,707,000	5.8	Bar Built	60°	1.361	41.0%
7	**Glaslyn**	15.70km^2	37,554,000	5.3	Bar Built	39°	1.343	22.2%
8	**Dee**	108.21km^2	576,536,000	3.5	Coastal Plain	136°	1.158	19.5%

[a] Tidal prism measured from hydrodynamic tidal models as the difference in water volume between MHWS and MLWS within estuary boundaries; [b] Tidal range data from UK Hydrographic Office (UKHO); [c] Estuary type data from enhanced FutureCoast project (UK Department for Environment, Food and Rural Affairs [DEFRA]) data[86]; [d] Measured orientation of estuary mouths, from Google Earth tools;[e] Estuary sinuosity measured using QGIS after the methodology of Schumm[87]; [f] Saltmarsh area calculated from data from Natural Resources Wales, under Open Government licence - Available at http://lle.gov.wales/catalogue/item/SaltmarshExtents.

Experimental design

For each of the case-study estuaries we used high-resolution hydrodynamic models to investigate how marsh vegetation state changes estuary hydrodynamics and resulting simulated flooding. We created online coupled Delft3D FLOW and WAVE (SWAN Cycle III 41.31) models[88], incorporating the effect of vegetation using a ridged cylinders approach[89] (Delft/SWAN-VEG) on both waves and flow. This approach has been successfully applied in recent numerical modelling studies which include vegetation[90,91], and has been found to be more consistent across contexts than fixed Manning's *n* friction approaches[92]. The hydrodynamic processes within Delft3D were calculated using a 2-dimensional depth-averaged form of the unsteady shallow water equations[93] which has been extensively utilised

and validated across a variety of applications and timescales[94–96], including for investigating the role of saltmarsh systems[90,91].

Models were run on high resolution structured grids. Offshore areas were typically represented as 150x50m grids, and grid sizes became progressively smaller towards the estuary mouth and the upstream areas. Grids within estuary boundaries were high resolution and uniform, with 10x10m cell sizes giving good resolution to resolve hydrodynamics in up-stream river channels and marsh creeks. The model domain extended into the terrestrial zone to 3m elevation above the height of the terrestrial-estuary boundary to characterise terrestrial flood extents and depths. Models were validated using a combination of tidal gauge (British Oceanographic Data Centre - BODC) and HOBO Depth logger (U20L) data deployed in each estuary group, and performed well against observed water levels in estuaries (see supplementary validation section - 3.2.4 - for additional information).

We used three different vegetation states: an unvegetated reference state, an undisturbed fully vegetated state where marsh platforms were fully populated with climax marsh communities, and a Grazed state where vegetation height was reduced to a uniform 8cm in line with field observations. Marsh vegetation properties were specified using Community Weighted Means (CWM) of plant trait data from vegetation surveys carried out as part of the CoastWEB project[31,90] (Supplementary table S15).

We also investigated how storm magnitude may change the relationship between vegetation and flood mitigation, as previous studies have indicated that vegetation may become less effective at attenuating energy with increased water levels from surge during larger storms[47], and larger storms are more frequently associated with significant flood events[23,97,98]. We used 3 storm events with increasing magnitudes; an annually expected 1 in 1 year storm event, a 1 in 10-year storm event, and a 1 in 100-year event. These storm events were constructed and calibrated by fitting observed surge[99], wave (Centre for Environment Fisheries & Aquaculture Science - CEFAS), United Kingdom wave hindcast dataset), wind (Met Office, UK) and river

401 flow data (Natural Resources Wales - NRW) using a Generalised Pareto Distribution (GPD)[100]
402 to determine significant storm conditions corresponding to each of the return periods.

403 To understand the roles and potential interactions of vegetation and storms, we used a fully
404 crossed factorial design, co-varying the vegetation state and storm magnitude over the 8
405 estuaries, creating 72 individual scenarios. We suspected that in estuaries, flood risk would
406 be dictated by different processes operating at different spatial scales, and so we analysed
407 depths, flood extents, current velocities and significant wave heights for each estuary and
408 scenario at three different spatial grains; local (transect level), segment (1km segments) and
409 whole estuary levels.

410 Previous studies have indicated that over-marsh transformation of waves and surge is the
411 most important pathway for reducing flooding in open-coastline systems[26,49,63]. To assess
412 whether this also applies in estuarine environments we employed transect sampling to look at
413 wave and surge transformation across individual marshes to examine the importance of marsh
414 vegetation for preventing flooding from local wave and surge overtopping of banks and
415 defences. Transects were created in QGIS and were mapped onto model output data at 250m
416 intervals, and sampling points were equally spaced at 10m intervals from the marsh/channel
417 edge until the terrestrial boundary. At each transect point we measured maximum water level,
418 significant wave height and current velocity. From this data, we then examined the total
419 reduction and proportional reduction in water level and wave height driven by the vegetation
420 from the channel to terrestrial boundary as an indicator of the effectiveness of marshes in
421 reducing local storm flooding.

422 We also suspected that vegetation may play a wider role in estuaries, creating a cumulative
423 drag effect at the estuary scale which could reduce flood extents further upstream[69]. To
424 investigate whether cumulative drag had a strong effect on flood potential, we decomposed
425 the model outputs into 1km sections along main estuary channels, and measured averaged
426 peak current velocity, averaged peak water level, and averaged peak significant wave height
427 within the estuary area sections, and flood extents and depths in adjacent terrestrial areas

using zonal statistics. These 1km sections extended from the estuary/coastal boundary, up until the limit of tidal intrusion (LTI). Because of the high degree of variability in absolute area and topography within estuaries, we calculated flood extents, water levels and depth within each block as a proportion of the maximum observed flood extent, levels or depth respectively within each estuary to look at the relative role of marsh vegetation independent of estuary context. We also applied this to the distance of sections upstream, as the estuaries varied considerably in length, with distance being represented as a proportion of distance of each section upstream from the estuary mouth (0) to the LTI (1). At the whole estuary level, we quantified average peak water level, mean peak current velocity (flood and ebb) and mean peak significant wave height using zonal statistics within the boundaries of the whole estuary. Additional information on model specification is available in the supplementary materials (section 3.1 to 3.2).

Economic Analysis

In addition to examining the hydrodynamic consequences of vegetation, we assessed the economic costs associated with flood events based on the extents and depths of flood waters from the hydrodynamic models. We compared the flood damages experienced in each estuary when marshes have no vegetation to those with full or grazed vegetation, and for different storm return levels (1 in 1, 1 in 10, 1 in 100 year). Our calculations aggregated flood damage estimates for residential, commercial, industrial and agricultural properties, as well as to public buildings and water and electricity utility installations using flood cost estimates for saltwater inundation damages (to building fabric, household inventory and domestic clean-up) from cost tables in the 2018 update of the Multi-Coloured Manual (MCM)[101]. Properties in at-risk areas were identified using OS Mastermap layers[102], assigned a building type (e.g. terraced, detached, retail properties etc.) and property age using a systematic visual assessment in Google StreetView©, and segmented by neighbourhood for socioeconomic status (UK Census Data[103]) to calculate economic cost values (in GBP(£)).

We also accounted for losses in agricultural output on flooded farmland, flosses from disruption to travel arising from flooded roads, and from restrictions in outdoor recreation activity resulting from the flooding of parks and countryside paths. Roads were identified using the Ordinance Survey Integrated Transport Network[104] data layer, and assigned a value for the average number of vehicles using them per hour from Department for Transport road traffic statistics data (DfT, 2020[105]). To calculate economic costs from flooding we applied a 'diversion-value method'[101], whereby vehicles were assumed to have to divert to avoid flooding. For the sake of simplicity, we assumed that diversion to extend the journey by a distance equal to the length of road made impassable by the flood water for a period of 12 hours. Travel disruption costs were then calculated by multiplying the costs per kilometre of additional travel - provided in the MCM cost tables[101] - by the number of vehicles affected during the flooding event. Estimates of flood losses arising in agriculture and outdoor recreation activity were also calculated, following established repair and disruption values in the Green Book (Central government guidance on appraisal and evaluation)[106].

We calculated absolute flood damage costs for single storms for each return-level event, as well as an annualised cost based on the Net Present Value (NPV)[101], and these values (in £GBP) were subsequently converted into $USD (at exchange rate of USD$1.36 to GBP£1; December 20th, 2020). As the exposure of assets varied between estuaries, we also recalculated these absolute values as proportional reductions, comparing the cost for each scenario with the maximum observed flood cost for each estuary. This allowed us to compare the relative flood protection value of marshes across estuaries, independently of population density and asset exposure. Further details on the economic analysis are available in the supplementary materials (Section 3.3)

Statistical analysis

Analysis of model outputs was conducted in the R statistical computing environment[107]. To analyse relative extent, water level and wave reduction (relative flood effects) data (proportional data) we employed mixed effects beta regression models using the glmmTMB

package[108] with the estuary as a random factor to account for unquantified environmental differences in prevailing conditions between estuaries. We assessed effects of a range of different predictors on flood effects at three different scales: Transect level (within marshes), up-stream zone, and whole estuary level. The proportional upstream distance and marsh width predictors were log10 transformed - at the estuary scale and marsh transect levels respectively - to account for non-linearity, and model diagnostics performed to ensure adequate model fit. Results were then visualised using the GGplot2[109], Coefplot[110] and Visreg[111] packages.

Acknowledgements

The authors would like to thank the members of the CoastWEB team for their support and feedback, Dr Davide de Battisti and Dr Thomas J. van Veelen for their valuable field assistance, as well as the anonymous reviewers that helped improve this manuscript. This research formed part of the Valuing Nature Programme (valuing-nature.net) which is funded by the Natural Environment Research Council, the Economic and Social Research Council, the Biotechnology and Biological Sciences Research Council, the Arts and Humanities Research Council and the Department of the Environment, Food and Rural Affairs. This research was supported by the UK Research Councils under Natural Environment Research Council award NE/N013573/1, Title CoastWEB: Valuing the contribution which COASTal habitats make to human health and WEllBeing, with a focus on the alleviation of natural hazards.

Author Contributions

TF and JG conceptualised the study, with input from HK, WB, NB, IM, MS, BD and GS. Experimental design was led by TF, with input from JG, HK, and WB, and hydrodynamic modelling was undertaken by TF with the assistance of WB. Analysis of model outputs was led by TF, with input from JG. TF undertook field sampling for vegetation and validation data.

Economic modelling was led by BD and GS, with input from TF and JG. TF and JG led the writing of the manuscript, with input from all co-authors.

Conflicts of Interest

The authors declare that they have no known competing financial interests or personal relationships that could have appeared to influence the work reported in this paper.

Data Availability Statement

The data that support the findings of this study will be openly available following publication at the following URL/DOI: 10.6084/m9.figshare.c.5461350

Supplementary Materials

Additional supporting information can be found in the Supplementary Materials

References

1. Kulp, S. A. & Strauss, B. H. New elevation data triple estimates of global vulnerability to sea-level rise and coastal flooding. *Nature Communications* **10**, 4844 (2019).
2. Hallegatte, S., Green, C., Nicholls, R. J. & Corfee-Morlot, J. Future flood losses in major coastal cities. *Nature Climate Change* **3**, 802–806 (2013).
3. Vitousek, S. *et al.* Doubling of coastal flooding frequency within decades due to sea-level rise. *Scientific Reports* **7**, 1399 (2017).
4. Kirezci, E. *et al.* Projections of global-scale extreme sea levels and resulting episodic coastal flooding over the 21st Century. *Scientific Reports* **10**, 11629 (2020).
5. Muis, S., Güneralp, B., Jongman, B., Aerts, J. C. J. H. & Ward, P. J. Flood risk and adaptation strategies under climate change and urban expansion: A probabilistic analysis using global data. *Science of The Total Environment* **538**, 445–457 (2015).
6. Neumann, B., Vafeidis, A. T., Zimmermann, J. & Nicholls, R. J. Future Coastal Population Growth and Exposure to Sea-Level Rise and Coastal Flooding - A Global Assessment. *PLOS ONE* **10**, e0118571 (2015).
7. McGranahan, G., Balk, D. & Anderson, B. The rising tide: assessing the risks of climate change and human settlements in low elevation coastal zones. *Environment and Urbanization* **19**, 17–37 (2007).
8. Mousavi, M. E., Irish, J. L., Frey, A. E., Olivera, F. & Edge, B. L. Global warming and hurricanes: the potential impact of hurricane intensification and sea level rise on coastal flooding. *Climatic Change* **104**, 575–597 (2011).
9. Emanuel, K. Increasing destructiveness of tropical cyclones over the past 30 years. *Nature* **436**, 686–688 (2005).
10. Webster, P. J., Holland, G. J., Curry, J. A. & Chang, H.-R. Changes in Tropical Cyclone Number, Duration, and Intensity in a Warming Environment. *Science* **309**, 1844–1846 (2005).

11. Wang, S. & Toumi, R. Recent migration of tropical cyclones toward coasts. *Science* **371**, 514–517 (2021).
12. Nott, J., Green, C., Townsend, I. & Callaghan, J. The World Record Storm Surge and the Most Intense Southern Hemisphere Tropical Cyclone: New Evidence and Modeling. *Bull. Amer. Meteor. Soc.* **95**, 757–765 (2014).
13. McRobie, A., Spencer, T. & Gerritsen, H. The big flood: North Sea storm surge. *Philosophical Transactions of the Royal Society A: Mathematical, Physical and Engineering Sciences* **363**, 1263–1270 (2005).
14. Rahmstorf, S. Rising hazard of storm-surge flooding. *Proceedings of the National Academy of Sciences* **114**, 11806–11808 (2017).
15. Muis, S., Verlaan, M., Winsemius, H. C., Aerts, J. C. J. H. & Ward, P. J. A global reanalysis of storm surges and extreme sea levels. *Nature Communications* **7**, 11969 (2016).
16. Valle-Levinson, A., Olabarrieta, M. & Heilman, L. Compound flooding in Houston-Galveston Bay during Hurricane Harvey. *Science of The Total Environment* **747**, 141272 (2020).
17. Lagmay, A. M. F. *et al.* Devastating storm surges of Typhoon Haiyan. *International Journal of Disaster Risk Reduction* **11**, 1–12 (2015).
18. Sibley, A., Cox, D. & Titley, H. Coastal flooding in England and Wales from Atlantic and North Sea storms during the 2013/2014 winter. *Weather* **70**, 62–70 (2015).
19. Kendon, M. & McCarthy, M. The UK's wet and stormy winter of 2013/2014. *Weather* **70**, 40–47 (2015).
20. Hinkel, J. *et al.* Coastal flood damage and adaptation costs under 21st century sea-level rise. *PNAS* **111**, 3292–3297 (2014).
21. Plate, E. J. Flood risk and flood management. *Journal of Hydrology* **267**, 2–11 (2002).
22. Marsalek, J., Stancalie, G. & Balint, G. *Transboundary floods: Reducing risks through flood management*. vol. 72 (Springer Science & Business Media, 2006).

23. Schanze, J. Flood risk management–a basic framework. in *Flood risk management: hazards, vulnerability and mitigation measures* 1–20 (Springer, 2006).
24. Zhu, Z. *et al.* Historic storms and the hidden value of coastal wetlands for nature-based flood defence. *Nature Sustainability* **3**, 853–862 (2020).
25. Vuik, V., Jonkman, S. N., Borsje, B. W. & Suzuki, T. Nature-based flood protection: The efficiency of vegetated foreshores for reducing wave loads on coastal dikes. *Coastal Engineering* **116**, 42–56 (2016).
26. Shepard, C. C., Crain, C. M. & Beck, M. W. The Protective Role of Coastal Marshes: A Systematic Review and Meta-analysis. *PLOS ONE* **6**, e27374 (2011).
27. Vuik, V., Borsje, B. W., Willemsen, P. W. J. M. & Jonkman, S. N. Salt marshes for flood risk reduction: Quantifying long-term effectiveness and life-cycle costs. *Ocean & Coastal Management* **171**, 96–110 (2019).
28. Guichard, F. & Bourget, E. Topographic heterogeneity, hydrodynamics, and benthic community structure: a scale-dependent cascade. *Marine Ecology Progress Series* **171**, 59–70 (1998).
29. Kumbier, K., Cabral Carvalho, R., Vafeidis, A. T. & Woodroffe, C. D. Investigating compound flooding in an estuary using hydrodynamic modelling: a case study from the Shoalhaven River, Australia. (2018).
30. Marsooli, R., Orton, P. M., Georgas, N. & Blumberg, A. F. Three-dimensional hydrodynamic modeling of coastal flood mitigation by wetlands. *Coastal Engineering* **111**, 83–94 (2016).
31. van Veelen, T. J., Fairchild, T. P., Reeve, D. E. & Karunarathna, H. Experimental study on vegetation flexibility as control parameter for wave damping and velocity structure. *Coastal Engineering* **157**, 103648 (2020).
32. Augustin, L. N., Irish, J. L. & Lynett, P. Laboratory and numerical studies of wave damping by emergent and near-emergent wetland vegetation. *Coastal Engineering* **56**, 332–340 (2009).

33. Hanslow, D. J., Morris, B. D., Foulsham, E. & Kinsela, M. A. A Regional Scale Approach to Assessing Current and Potential Future Exposure to Tidal Inundation in Different Types of Estuaries. *Scientific Reports* **8**, 7065 (2018).

34. Pye, K. & Blott, S. J. The geomorphology of UK estuaries: The role of geological controls, antecedent conditions and human activities. *Estuarine, Coastal and Shelf Science* **150**, 196–214 (2014).

35. Monbaliu, J. *et al.* Risk assessment of estuaries under climate change: Lessons from Western Europe. *Coastal Engineering* **87**, 32–49 (2014).

36. Spicer, P., Huguenard, K., Ross, L. & Rickard, L. N. High-Frequency Tide-Surge-River Interaction in Estuaries: Causes and Implications for Coastal Flooding. *Journal of Geophysical Research: Oceans* **124**, 9517–9530 (2019).

37. Ward, P. J. *et al.* Dependence between high sea-level and high river discharge increases flood hazard in global deltas and estuaries. *Environmental Research Letters* **13**, 084012 (2018).

38. Lyddon, C., Brown, J. M., Leonardi, N. & Plater, A. J. Flood Hazard Assessment for a Hyper-Tidal Estuary as a Function of Tide-Surge-Morphology Interaction. *Estuaries and Coasts* **41**, 1565–1586 (2018).

39. Prime, T., Brown, J. M. & Plater, A. J. Physical and Economic Impacts of Sea-Level Rise and Low Probability Flooding Events on Coastal Communities. *PLOS ONE* **10**, e0117030 (2015).

40. Gibson, R. N., Atkinson, R. J. A. & Gordon, J. D. M. *Oceanography and Marine Biology: An Annual Review, Volume 48*. (CRC Press, 2010).

41. Narayan, S. *et al.* The Value of Coastal Wetlands for Flood Damage Reduction in the Northeastern USA. *Scientific Reports* **7**, 9463 (2017).

42. Temmerman, S. *et al.* Ecosystem-based coastal defence in the face of global change. *Nature* **504**, 79–83 (2013).

43. Silliman, B. R., Grosholz, E. D. & Bertness, M. D. *Human Impacts on Salt Marshes: A Global Perspective*. (University of California Press, 2009).

618 44. Thorne, K. *et al.* U.S. Pacific coastal wetland resilience and vulnerability to sea-level rise.
619 *Science Advances* **4**, eaao3270 (2018).
620 45. Li, X., Bellerby, R., Craft, C. & Widney, S. E. Coastal wetland loss, consequences, and challenges
621 for restoration. *Anthropocene Coasts* (2018) doi:10.1139/anc-2017-0001.
622 46. Temmerman, S., De Vries, M. B. & Bouma, T. J. Coastal marsh die-off and reduced attenuation
623 of coastal floods: A model analysis. *Global and Planetary Change* **92–93**, 267–274 (2012).
624 47. Möller, I. *et al.* Wave attenuation over coastal salt marshes under storm surge conditions.
625 *Nature Geoscience* **7**, 727–731 (2014).
626 48. Yang, S. L., Shi, B. W., Bouma, T. J., Ysebaert, T. & Luo, X. X. Wave Attenuation at a Salt Marsh
627 Margin: A Case Study of an Exposed Coast on the Yangtze Estuary. *Estuaries and Coasts* **35**,
628 169–182 (2012).
629 49. Wamsley, T. V., Cialone, M. A., Smith, J. M., Atkinson, J. H. & Rosati, J. D. The potential of
630 wetlands in reducing storm surge. *Ocean Engineering* **37**, 59–68 (2010).
631 50. Paul, M. *et al.* Plant parameters as drivers for drag forces under extreme wave loading. *11th*
632 *International Symposium on Ecohydraulics (ISE 2016)* 43 (2016).
633 51. Tanino, Y. & Nepf, H. M. Laboratory Investigation of Mean Drag in a Random Array of Rigid,
634 Emergent Cylinders. *Journal of Hydraulic Engineering* **134**, 34–41 (2008).
635 52. Paquier, A.-E., Haddad, J., Lawler, S. & Ferreira, C. M. Quantification of the Attenuation of
636 Storm Surge Components by a Coastal Wetland of the US Mid Atlantic. *Estuaries and Coasts* **40**,
637 930–946 (2017).
638 53. Smolders, S. *et al.* Modeling Storm Surge Attenuation by an Integrated Nature-Based and
639 Engineered Flood Defense System in the Scheldt Estuary (Belgium). *Journal of Marine Science*
640 *and Engineering* **8**, 27 (2020).
641 54. Stark, J., Oyen, T. V., Meire, P. & Temmerman, S. Observations of tidal and storm surge
642 attenuation in a large tidal marsh. *Limnology and Oceanography* **60**, 1371–1381 (2015).

643 55. Loder, N. M., Irish, J. L., Cialone, M. A. & Wamsley, T. V. Sensitivity of hurricane surge to
644 morphological parameters of coastal wetlands. *Estuarine, Coastal and Shelf Science* **84**, 625–
645 636 (2009).
646 56. Gilbertson, N. M., Adams, T. P. & Burrows, M. T. From marshes to coastlines: A metric for local
647 and national scale identification of high-value habitat for coastal protection. *Estuarine, Coastal*
648 *and Shelf Science* **246**, 107022 (2020).
649 57. Rezaie, A. M., Loerzel, J. & Ferreira, C. M. Valuing natural habitats for enhancing coastal
650 resilience: Wetlands reduce property damage from storm surge and sea level rise. *PLOS ONE*
651 **15**, e0226275 (2020).
652 58. Hodgkin, E. P. & Lenanton, R. C. Estuaries and Coastal Lagoons of South Western Australia. in
653 *Estuaries and Nutrients* (eds. Neilson, B. J. & Cronin, L. E.) 307–321 (Humana Press, 1981).
654 doi:10.1007/978-1-4612-5826-1_14.
655 59. Roy, P. S. *et al.* Structure and Function of South-east Australian Estuaries. *Estuarine, Coastal*
656 *and Shelf Science* **53**, 351–384 (2001).
657 60. Emmett, R. *et al.* Geographic signatures of North American West Coast estuaries. *Estuaries* **23**,
658 765–792 (2000).
659 61. Dubarbier, B., Castelle, B., Marieu, V. & Ruessink, G. Process-based modeling of cross-shore
660 sandbar behavior. *Coastal Engineering* **95**, 35–50 (2015).
661 62. Hu, X., Yang, F., Song, L. & Wang, H. An Unstructured-Grid Based Morphodynamic Model for
662 Sandbar Simulation in the Modaomen Estuary, China. *Water* **10**, 611 (2018).
663 63. Möller, I., Spencer, T., French, J. R., Leggett, D. J. & Dixon, M. Wave Transformation Over Salt
664 Marshes: A Field and Numerical Modelling Study from North Norfolk, England. *Estuarine,*
665 *Coastal and Shelf Science* **49**, 411–426 (1999).
666 64. Mury, A., Collin, A., Houet, T., Alvarez-Vanhard, E. & James, D. Using Multispectral Drone
667 Imagery for Spatially Explicit Modeling of Wave Attenuation through a Salt Marsh Meadow.
668 *Drones* **4**, 25 (2020).

669 65. Zhang, X., Lin, P., Gong, Z., Li, B. & Chen, X. Wave Attenuation by Spartina alterniflora under
670 Macro-Tidal and Storm Surge Conditions. *Wetlands* (2020) doi:10.1007/s13157-020-01346-w.
671 66. Dronkers, J. Tidal asymmetry and estuarine morphology. *Netherlands Journal of Sea Research*
672 **20**, 117–131 (1986).
673 67. Tajima, Y., Hamada, Y. & Hussain, M. A. Impact of Dynamic Morphology Change on Storm
674 Surge Disaster Risks along the Meghna Estuary. *Procedia Engineering* **116**, 947–954 (2015).
675 68. Spicer, P. Tide and Storm Surge Dynamics in Estuaries of Variable Morphology. (2019).
676 69. Smolders, S., Plancke, Y., Ides, S., Meire, P. & Temmerman, S. Role of intertidal wetlands for
677 tidal and storm tide attenuation along a confined estuary: a model study. *Natural Hazards and*
678 *Earth System Sciences* **15**, 1659–1659 (2015).
679 70. Dürr, H. H. *et al.* Worldwide Typology of Nearshore Coastal Systems: Defining the Estuarine
680 Filter of River Inputs to the Oceans. *Estuaries and Coasts* **34**, 441–458 (2011).
681 71. Lyddon, C., Brown, J. M., Leonardi, N. & Plater, A. J. Uncertainty in estuarine extreme water
682 level predictions due to surge-tide interaction. *PLOS ONE* **13**, e0206200 (2018).
683 72. Sun, F. & Carson, R. T. Coastal wetlands reduce property damage during tropical cyclones.
684 *PNAS* **117**, 5719–5725 (2020).
685 73. Costanza, R. *et al.* The Value of Coastal Wetlands for Hurricane Protection. *ambi* **37**, 241–248
686 (2008).
687 74. Barbier, E. B. Valuing the storm protection service of estuarine and coastal ecosystems.
688 *Ecosystem Services* **11**, 32–38 (2015).
689 75. Lockwood, B. & Drakeford, B. M. The value of carbon sequestration by saltmarsh in Chichester
690 Harbour, United Kingdom. *Journal of Environmental Economics and Policy* **0**, 1–15 (2021).
691 76. Beaumont, N. J., Jones, L., Garbutt, A., Hansom, J. D. & Toberman, M. The value of carbon
692 sequestration and storage in coastal habitats. *Estuarine, Coastal and Shelf Science* **137**, 32–40
693 (2014).

694 77. King, S. E. & Lester, J. N. The value of salt marsh as a sea defence. *Marine Pollution Bulletin* **30**,
695 180–189 (1995).
696 78. Barbier, E. B. *et al.* The value of estuarine and coastal ecosystem services. *Ecological*
697 *Monographs* **81**, 169–193 (2011).
698 79. Silliman, B. R. *et al.* Field Experiments and Meta-analysis Reveal Wetland Vegetation as a
699 Crucial Element in the Coastal Protection Paradigm. *Current Biology* **29**, 1800-1806.e3 (2019).
700 80. Leonardi, N. *et al.* Dynamic interactions between coastal storms and salt marshes: A review.
701 *Geomorphology* **301**, 92–107 (2018).
702 81. Narayan, S. *et al.* The Effectiveness, Costs and Coastal Protection Benefits of Natural and
703 Nature-Based Defences. *PLOS ONE* **11**, e0154735 (2016).
704 82. Möller, I. Applying Uncertain Science to Nature-Based Coastal Protection: Lessons From
705 Shallow Wetland-Dominated Shores. *Front. Environ. Sci.* **7**, (2019).
706 83. Li, M., Zhang, F., Barnes, S. & Wang, X. Assessing storm surge impacts on coastal inundation
707 due to climate change: case studies of Baltimore and Dorchester County in Maryland. *Nat*
708 *Hazards* **103**, 2561–2588 (2020).
709 84. Oppenheimer, M. *et al. Sea Level Rise and Implications for Low-Lying Islands, Coasts and*
710 *Communities*. (2019).
711 85. Alder, J. Putting the coast in the “Sea Around Us”. *The Sea Around Us Newsletter* **15**, 1–2
712 (2003).
713 86. Manning, A. J. Enhanced UK estuaries database: Explanatory notes and metadata. in *Technical*
714 *Report TR167, HR Wallingford Tech. Report, TR167, UK* (2007).
715 87. Schumm, S. A. Sinuosity of Alluvial Rivers on the Great Plains. *GSA Bulletin* **74**, 1089–1100
716 (1963).
717 88. Lesser, G. R., Roelvink, J. v, Van Kester, J. & Stelling, G. S. Development and validation of a
718 three-dimensional morphological model. *Coastal engineering* **51**, 883–915 (2004).

89. Dalrymple, R. A., Kirby, J. T. & Hwang, P. A. Wave Diffraction Due to Areas of Energy Dissipation. *Journal of Waterway, Port, Coastal, and Ocean Engineering* **110**, 67–79 (1984).
90. Bennett, W. G., van Veelen, T. J., Fairchild, T. P., Griffin, J. N. & Karunarathna, H. Computational Modelling of the Impacts of Saltmarsh Management Interventions on Hydrodynamics of a Small Macro-Tidal Estuary. *Journal of Marine Science and Engineering* **8**, 373 (2020).
91. Ashall, L. M., Mulligan, R. P., van Proosdij, D. & Poirier, E. Application and validation of a three-dimensional hydrodynamic model of a macrotidal salt marsh. *Coastal Engineering* **114**, 35–46 (2016).
92. Wang, J. & Zhang, Z. Evaluating Riparian Vegetation Roughness Computation Methods Integrated within HEC-RAS. *Journal of Hydraulic Engineering* **145**, 04019020 (2019).
93. Roelvink, J. A. & Van Banning, G. Design and development of DELFT3D and application to coastal morphodynamics. *Oceanographic Literature Review* **11**, 925 (1995).
94. Elias, E. P. L., Walstra, D. J. R., Roelvink, J. A., Stive, M. J. F. & Klein, M. D. Hydrodynamic Validation of Delft3D with Field Measurements at Egmond. 2714–2727 (2012) doi:10.1061/40549(276)212.
95. Symonds, A. M. *et al.* Comparison between Mike 21 FM, Delft3D and Delft3D FM flow models of western port bay, Australia. *COASTAL ENGINEERING* 2 (2016).
96. Hsu, Y. L., Dykes, J. D., Allard, R. A. & Kaihatu, J. M. *Evaluation of Delft3D performance in nearshore flows*. (2006).
97. Lapetina, A. & Sheng, Y. P. Three-Dimensional Modeling of Storm Surge and Inundation Including the Effects of Coastal Vegetation. *Estuaries and Coasts* **37**, 1028–1040 (2014).
98. Li, A. *et al.* Modeling wave effects on storm surge from different typhoon intensities and sizes in the South China Sea. *Estuarine, Coastal and Shelf Science* **235**, 106551 (2020).
99. McMillan, A. *et al. Coastal Flood Boundary Conditionsfor UK Mainland and Islands*. (2011).
100. Hawkes, P. J., Gouldby, B. P., Tawn, J. A. & Owen, M. W. The joint probability of waves and water levels in coastal engineering design. *Journal of Hydraulic Research* **40**, 241–251 (2002).

101. Penning-Rowsell, E. *et al. Flood and Coastal Erosion Risk Management A Manual for Economic Appraisal*. (2013).
102. Ordinance Survey. OS MasterMap Topography Layer. https://www.ordnancesurvey.co.uk/business-government/products/mastermap-topography.
103. Gale, C. G., Singleton, A. D., Bates, A. G. & Longley, P. A. Creating the 2011 area classification for output areas (2011 OAC). *Journal of Spatial Information Science* **2016**, 1–27 (2016).
104. Ordinance Survey. OS MasterMap Highways Network Roads. https://www.ordnancesurvey.co.uk/business-government/tools-support/mastermap-highways-support.
105. UK Department for Transport. Road traffic statistics. https://roadtraffic.dft.gov.uk/downloads.
106. Treasury, H. M. The green book: Central government guidance on appraisal and evaluation. *London: HM Treasury* (2018).
107. R Core Team. *R: A Language and Environment for Statistical Computing*. (R Foundation for Statistical Computing, 2013).
108. Magnusson, A. *et al.* Package 'glmmTMB'. *R Package Version 0.2. 0* (2017).
109. Wickham, H. *ggplot2: elegant graphics for data analysis*. (springer, 2016).
110. Lander, J. P. *coefplot: Plots Coefficients from Fitted Models*. (2016).
111. Breheny, P. & Burchett, W. *visreg: Visualization of Regression Models*. (2016).

Supporting Information

Coastal wetlands mitigate storm flooding and associated costs in estuaries

Table of Contents:

1: Systematic Literature Review:

To better understand the state of knowledge around the role of saltmarshes in reducing potential flooding, we conducted a systematic review of the literature. Searches were conducted using the Boolean search terms [("Surge" OR "Wave") AND ("Wetland" OR "marsh" OR "Saltmarsh") AND ("attenuation" OR "reduction" OR "mitigation") AND “coastal”] between 1970-2020 on Google Scholar, ISI Web of Science, and Science Direct to identify potential research articles for inclusion and reference lists were checked to identify additional relevant articles. Returned articles were then filtered to only include articles which explicitly examined the role of saltmarsh vegetation on resulting wave or surge attenuation, other aquatic vegetative ecosystems (e.g. mangrove or seagrass systems), or small-scale fluid-dynamics modelling studies of vegetation stems were rejected. Of the 284 unique articles returned by searches, 26 met the criteria for inclusion. For each article, the type of study (hydrodynamic/ numerical modelling, observational studies or experimental manipulation) was identified, along with the scale (local area or regional) of the study. We then identified whether studies had considered the role of marsh vegetation for; localised, direct over-marsh attenuation of waves or surge, potential far-field upstream attenuation, or resulting flood extents and impacts, as well as the type of coastline considered and whether the study explicitly examined the specific role of vegetation by having unvegetated reference states. The results from the systematic review are presented in table S1, as well as visually represented in figure 1b in the main article.

Supplementary Table S1: Systematic review of the role of saltmarshes in reducing flood impacts from waves or surge, highlighting the gap in our understanding of the combined roles of wave and surge reduction across scales. Study types are grouped into categories, with the first part representing the study type ("HDM-" studies are from hydrodynamic model simulations, "OBS-" are observational studies and "EXP- " are experimental manipulations ex-situ), and the second part representing the scale at which the study has been undertaken ("-M" is at multiple scales (both local and estuary scales), "-L" is local-scale only, and "-R" are studies at regional scales only). Similarly, studies were grouped by coastline type: where "ES-S/M" represents small to medium sized estuaries, "ES-L" are large estuaries, "EMB" are embayments, "BB" are back-barrier marsh systems, "OP" are open coastline marsh systems, "LAG" are marsh systems in lagoons, and "SYN-OP" are synthetically created idealised marsh sections which are representative of open coastline conditions. ** included the role of surge in modifying wave attenuation, but did not measure surge attenuation per se.*

Study Type	Spatial Coverage	Direct Attenuation	Up-stream attenuation	Wave	Surge	Flooding	Unvegetated Comparison	Coastline Type	Country	Ref
HDM-M	**Transects + Whole estuary, 8 Estuaries**	**YES**	**YES**	**YES**	**YES**	**YES**	**YES**	**ES-S/M**	**UK**	**THIS STUDY**
HDM-L	Transects, Single Estuary	YES	NO	NO	YES	NO	YES	ES-L, EMB	USA	Wamsley et al., 2010[1]
HDM-L	Transects, Single Loci	YES	NO	YES	NO	NO	NO	SYN-OP	N/A Synthetic	Meijer, 2005[2]
HDM-L	Single Estuary Section	YES	ALONG CREEK	NO	YES	NO	NO	ES-L	Netherlands	Stark et al., 2016[3]
HDM-L	Transects, Single Loci	YES	NO	YES	NO	NO	YES	BB	Netherlands	van Loon-Steensma et al., 2016[4]
HDM-L	Single Coastline	YES	NO	NO	YES	NO	YES	EMB	USA	Loder et al., 2009[5]
HDM-L	Transects, Single Loci	YES	NO	NO	YES	NO	YES	OP	N/A Synthetic	Temmerman et al., 2012[6]
HDM-L	Transects, Single Estuary	YES	NO	NO	YES	NO	YES	EMB	USA	Hu et al., 2015[7]
HDM-L, OBS-L	Transects, Single Estuary	YES	NO	YES	NO	NO	YES	ES-L	Netherlands	Vuik et al., 2016[8]
HDM-R	Contiguous Coastline	YES	NO	NO*	NO*	YES	NO	ES-L	USA	Haddad et al., 2015[9]
HDM-R	Single Estuary	NO	YES	NO	YES	NO	YES	ES-L	Netherlands	Smolders et al., 2015[10]
HDM-R	Contiguous Coastline	YES	NO	NO	YES	YES	YES	ES-L, EMB	USA	Barbier et al., 2013[11]
HDM-R	Contiguous Coastline	YES	YES	NO	YES	YES	YES	ES-L, EMB, OP	USA	Narayan et al., 2017 [12]
OBS-L	Transects, Single Estuary	YES	ALONG CREEK	NO	YES	NO	NO	ES-L	Netherlands	Stark et al., 2015[13]
OBS-L	Transects, Single Estuary	YES	NO	YES	NO	NO	YES	ES-L, OP	China	Yang et al., 2012[14]
OBS-L	Transects, Single Estuary	YES	NO	YES	NO	NO	NO	ES-L, OP	China	Ysebaert et al., 2011[15]
OBS-L	Transects, Single Estuary	YES	NO	YES	YES	NO	NO	ES-L	USA	Paquier et al., 2017[16]
OBS-L	Transects, Single Estuary	YES	NO	YES	NO	NO	NO	EMB	USA	Foster-Martinez et al., 2018[17]
OBS-L	Transects, Single Estuary	YES	NO	YES	NO	NO	NO	LAG	USA	Jadhav and Chen, 2012[18]
OBS-L	Transects, Single Loci	YES	NO	YES	NO*	NO	NO	EMB	China	Zhang et al., 2020[19]
OBS-L	Transects, Two Loci	YES	NO	YES	NO	NO	NO	OP, BB	UK	Möller et al., 1999[20]
OBS-L	Transects, Single Estuary	YES	NO	YES	NO	NO	NO	ES-L	USA	Knutson et al., 1982[21]
OBS-L	Transects, Single Loci	YES	NO	YES	NO	NO	NO	OP	UK	Möller et al., 2006[22]
OBS-L	Transects, Two Loci	YES	NO	YES	NO	NO	YES	OP	UK	Möller & Spencer, 2002[23]
OBS-L	Transects, Single Loci	YES	NO	YES	NO	NO	NO	OP	UK	Cooper, 2005[24]
OBS-R	Transects, 10 Locations	YES	NO	YES	NO	NO	YES	OP, EMB	USA	Morgan et al., 2009[25]
EXP-L	Transects, Single Loci	YES	NO	YES	NO*	NO	YES	SYN-OP	N/A Synthetic	Möller et al., 2014[26]

2: Supplementary results

Supplementary Table S2: The positive role of marsh vegetation in reducing flood extents. Modelled terrestrial flooded extent (km^2) for each storm event, vegetation scenario and estuary, with the proportion of flood extent area relative to the maximum observed within the estuary in parentheses. The reduction in flood extents are also presented as a percent reduction by vegetation, relative to the unvegetated scenario (Relative Reduction).

Estuary	Event	Vegetated	Grazed	Unvegetated	Relative Reduction
Dee	1	2.165km² (0.56)	2.356km² (0.61)	2.407km² (0.62)	10.0%
	10	3.145km² (0.82)	3.268km² (0.85)	3.659km² (0.95)	14.0%
	100	3.444km² (0.89)	3.497km² (0.91)	3.854km² (**1.00**)	10.6%
Glaslyn	1	4.509km² (0.33)	4.678km² (0.35)	8.451km² (0.63)	46.6%
	10	7.337km² (0.54)	8.184km² (0.61)	11.368km² (0.84)	35.5%
	100	9.260km² (0.69)	10.981km² (0.82)	13.468km² (**1.00**)	31.2%
Gwendaerth	1	0.263km² (0.10)	0.455km² (0.16)	1.970km² (0.72)	86.6%
	10	0.508km² (0.18)	0.954km² (0.35)	2.450km² (0.91)	79.3%
	100	1.143km² (0.42)	1.913km² (0.69)	2.750km² (**1.00**)	58.4%
Loughor	1	3.971km² (0.55)	3.765km² (0.52)	4.733km² (0.65)	16.1%
	10	4.610km² (0.64)	4.973km² (0.69)	6.157km² (0.85)	25.1%
	100	5.813km² (0.80)	5.906km² (0.82)	7.246km² (**1.00**)	19.8%
Mawddach	1	1.027km² (0.38)	0.994km² (0.36)	1.028km² (0.38)	<0.01%
	10	1.883km² (0.69)	1.871km² (0.68)	2.243km² (0.82)	16.1%
	100	2.273km² (0.83)	2.250km² (0.82)	2.733km² (**1.00**)	16.8%
Neath	1	0.479km² (0.24)	0.538km² (0.27)	0.869km² (0.43)	56.6%
	10	1.067km² (0.53)	1.141km² (0.57)	1.459km² (0.72)	26.9%
	100	1.665km² (0.83)	1.733km² (0.86)	2.014km² (1.00)	17.3%
Taf	1	1.177km² (0.15)	1.124km² (0.15)	1.356km² (0.18)	13.2%
	10	2.199km² (0.28)	2.523km² (0.33)	3.707km² (0.47)	40.7%
	100	3.221km² (0.42)	3.609km² (0.47)	7.729km² (1.00)	58.3%
Towy	1	0.164km² (0.15)	0.221km² (0.20)	0.899km² (0.80)	81.7%
	10	0.567km² (0.50)	0.594km² (0.52)	1.007km² (0.90)	43.7%
	100	0.710km² (0.63)	0.820km² (0.73)	1.125km² (1.00)	36.9%

Supplementary Table S3: Marsh proportion and presence reduced flood extents, particularly during large storms. Mixed-effects beta-regression model summary of the effects of vegetation state, proportional saltmarsh area, tidal prism and estuary sinuosity on flood extent for different magnitude storms.

Storm Magnitude	Predictor	Estimate	S.E.	Z-value	P
1 in 1	Intercept	-0.445	0.121	-3.680	
	Vegetation	-0.112	0.153	-0.730	0.463
	Saltmarsh Proportion	-0.432	0.166	-2.610	**0.009****
	Tidal Prism	0.356	0.138	2.580	**0.009****
	Sinuosity	0.041	0.133	0.310	0.755
1 in 10	Intercept	0.618	0.106	5.840	
	Vegetation	-0.163	0.123	-1.320	0.185
	Saltmarsh Proportion	-0.552	0.127	-4.340	**<0.001*****
	Tidal Prism	0.337	0.134	2.520	**0.012***
	Sinuosity	-0.130	0.115	-1.130	0.259
1 in 100	Intercept	1.746	0.158	11.090	
	Vegetation	-0.413	0.154	-2.680	**0.008****
	Saltmarsh Proportion	-0.739	0.156	-4.750	**<0.001*****
	Tidal Prism	0.086	0.175	0.490	0.625
	Sinuosity	-0.172	0.147	-1.170	0.242

Supplementary Table S4: Marsh proportion and presence reduced estuary-scale flood depths, particularly during large storms. Statistical model summary of the effects of vegetation state, proportional saltmarsh area, tidal prism, and estuary sinuosity on flood depths for different magnitude storms.

Event	Predictor	Estimate	S.E.	Z-value	P
1	Intercept	-0.96	0.105	-9.140	
	Vegetation	-0.224	0.131	-1.710	0.088
	Saltmarsh Proportion	-0.274	0.137	-2.000	**0.046***
	Tidal Prism	0.457	0.109	4.190	**<0.001*****
	Sinuosity	0.152	0.107	1.420	0.155
10	Intercept	0.003	0.100	0.030	
	Vegetation	-0.177	0.124	-1.430	0.153
	Saltmarsh Proportion	-0.470	0.132	-3.570	**<0.001*****
	Tidal Prism	0.130	0.113	1.150	0.252
	Sinuosity	0.075	0.111	0.670	0.501
100	Intercept	1.220	0.174	7.010	
	Vegetation	-0.426	0.190	-2.240	0.025*
	Saltmarsh Proportion	-0.795	0.203	-3.930	<0.001***
	Tidal Prism	-0.066	0.184	-0.360	0.721
	Sinuosity	0.019	0.173	0.110	0.915

Supplementary Table S5: Absolute economic Cost in USD ($) for each return level flood event in each of the studied estuaries. The proportion of flood costs relative to the maximum observed within the estuary are presented in parentheses. The reduction in flood costs are also presented as a percent reduction by vegetation, relative to the unvegetated scenario (Relative Reduction).

Estuary	Event	Vegetated	Grazed	Unvegetated	Relative Reduction
Dee	1	741,389 (**0.04**)	748,521 (**0.04**)	846,660 (**0.04**)	18.9%
	10	972,446 (**0.05**)	1,023,941 (**0.05**)	1,172,298 (**0.06**)	17.0%
	100	20,525,272 (**1.00**)	18,773,367 (**0.91**)	19,151,840 (**0.93**)	-7.2%
Glaslyn	1	11,405,888 (**0.47**)	11,239,830 (**0.46**)	14,080,255 (**0.58**)	19.0%
	10	14,906,068 (**0.61**)	15,479,399 (**0.64**)	17,205,588 (**0.71**)	13.4%
	100	19,085,844 (**0.78**)	20,322,408 (**0.83**)	24,321,775 (**1.00**)	21.5%
Gwendaerth	1	226,137 (**0.04**)	310,223 (**0.06**)	2,729,451 (**0.54**)	91.7%
	10	658,286 (**0.13**)	737,589 (**0.15**)	4,851,947 (**0.96**)	86.4%
	100	721,313 (**0.14**)	2,890,137 (**0.57**)	5,031,895 (**1.00**)	85.7%
Loughor	1	27,216,780 (**0.29**)	25,679,302 (**0.27**)	32,381,332 (**0.35**)	15.9%
	10	32,968,084 (**0.35**)	34,593,229 (**0.37**)	49,772,910 (**0.53**)	33.8%
	100	55,846,542 (**0.60**)	58,721,312 (**0.63**)	93,508,450 (**1.00**)	40.3%
Mawddach	1	3,512,196 (**0.37**)	3,360,404 (**0.35**)	3,865,585 (**0.41**)	9.1%
	10	4,601,089 (**0.49**)	4,519,453 (**0.48**)	5,385,253 (**0.57**)	14.6%
	100	8,538,553 (**0.90**)	7,344,694 (**0.78**)	9,471,251 (**1.00**)	9.9%
Neath	1	774,695 (**0.03**)	204,558 (**0.01**)	782,866 (**0.03**)	1.0%
	10	1,641,912 (**0.07**)	1,637,603 (**0.07**)	1,753,762 (**0.07**)	6.4%
	100	6,319,308 (**0.27**)	5,684,524 (**0.24**)	23,714,089 (**1.00**)	73.4%
Taf	1	239,133 (**0.12**)	358,873 (**0.19**)	316,238 (**0.16**)	24.4%
	10	399,012 (**0.21**)	446,776 (**0.23**)	795,147 (**0.41**)	49.8%
	100	780,380 (**0.40**)	917,698 (**0.47**)	1,935,827 (**1.00**)	59.7%
Towy	1	157,974 (**0.06**)	966,420 (**0.36**)	656,482 (**0.25**)	75.9%
	10	747,287 (**0.28**)	850,026 (**0.32**)	2,237,577 (**0.84**)	66.6%
	100	865,569 (**0.32**)	2,090,271 (**0.78**)	2,668,690 (**1.00**)	67.6%

Supplementary Table S6: Annualised flood damage costs in USD ($) for fully vegetated, grazed and unvegetated marshes, demonstrating the positive role of marsh vegetation in reducing flooding costs. Parentheses in the vegetated and grazed scenarios represent percentage cost savings compared with the unvegetated reference state.

	Vegetated	Grazed	Unvegetated	Difference
Dee	1,943,877 (***3.5%***)	1,876,221 (***6.9%***)	2,014,634	70,757
Glaslyn	13,560,874 (***16.2%***)	13,837,957 (***14.5%***)	16,190,578	2,629,704
Gwendaerth	467,285 (***88.0%***)	663,664 (***83.0%***)	3,906,721	3,439,436
Loughor	31,638,312 (***28.7%***)	31,909,007 (***28.1%***)	44,352,154	12,713,842
Mawddach	4,327,648 (***12.2%***)	4,153,269 (***15.7%***)	4,926,132	598,484
Neath	1,508,921 (***40.2%***)	1,215,312 (***51.9%***)	2,524,677	1,015,756
Taf	348,041 (***45.8%***)	433,121 (***32.6%***)	642,376	294,335
Towy	488,602 (***68.5%***)	1,075,371 (***30.6%***)	1,549,795	1,061,193
	54,283,560	55,163,924	76,107,068	

Supplementary Table S7: Annualised flood damage cost savings per hectare, per year (ha/yr) in USD ($) (2020 values) and comparison with carbon storage and grazing land service values for UK saltmarshes, adjusted for inflation (Bank of England) at 2.7% PA between 1995-2020 (grazing value), and 2.9% PA between 2009-2020 (carbon value).

	Flood Saving (ha/yr)	Carbon Value (ha/yr)[A]	Grazing Value (ha/yr)[B]
Dee	$ 34	$64-220	$41
Glaslyn	$ 7,557		
Gwendaerth	$ 5,676		
Loughor	$ 5,813		
Mawddach	$ 2,733		
Neath	$11,162		
Taf	$ 873		
Towy	$ 4,331		
Average	$ 4,772	(SE±$1285)	

[A]From Beaumont et al., 2013[27]; [B]From King and Lester, 1995[28]. In 2020 values, accounting for inflation.

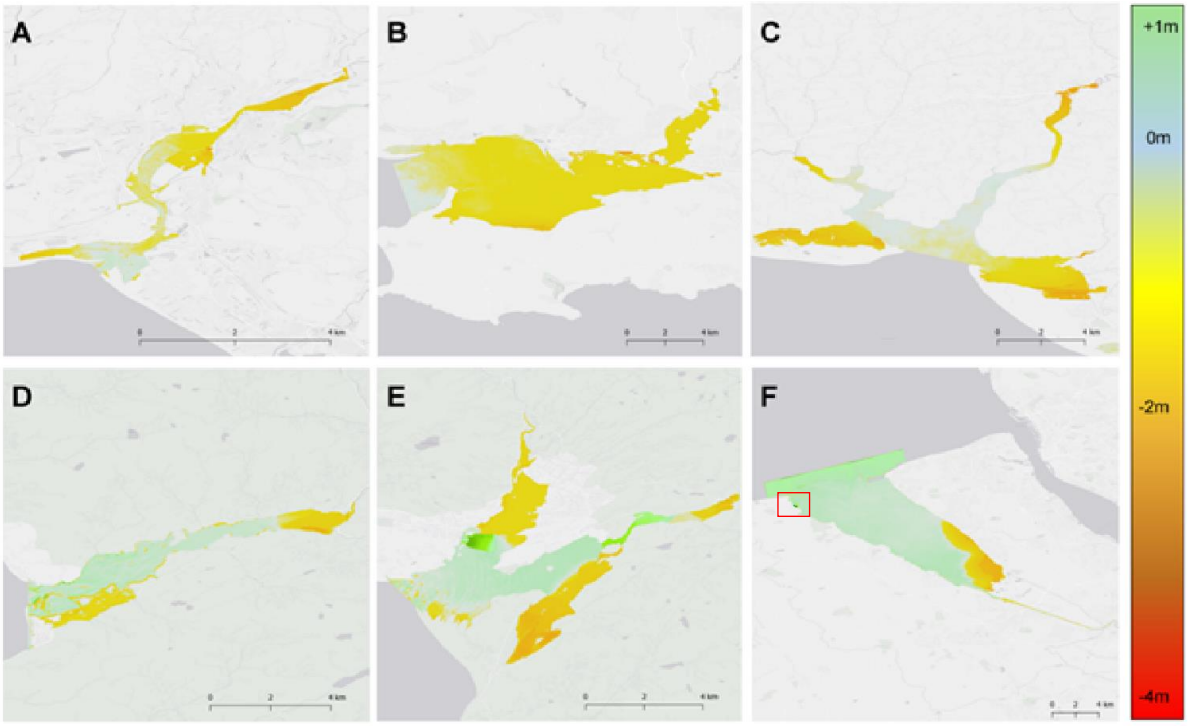

Supplementary Figure S1: Differences in water level between unvegetated and vegetated scenarios for a 1 in 100 Storm, illustrating the estuary-scale reductions in flooding of upstream areas by vegetation. Green colours (positive values) indicate enhancement of water level due to vegetation, and warmer yellows to reds (negative values) indicate water level reduction caused by vegetation. Results presented for the Neath (**A**), Loughor (**B**), Three Rivers Complex (Taf, Towy, Gwendraeth)(**C**), Mawddach (**D**), Glaslyn (**E**) and Dee (**F**) estuaries. The Red box on the Dee Estuary (**F**) indicates an industrial area that saw additional flooding when vegetation was present for a 100 year storm event. In units of meters (m).

Supplementary Table S8: Vegetation drives reductions in channel flood current velocity particularly with increasing distance upstream and during large storms. Statistical model summary of the effects of vegetation state, proportional distance upstream and their interaction on flood current velocity within 1km long estuary "zones".

Event	Predictor	Estimate	S.E.	Z-value	P
1	Intercept	0.710	0.258	2.750	
	Grazed Vegetation	-1.268	0.151	-8.410	**<0.001*** **
	Full Vegetation	-1.559	0.151	-10.310	**<0.001*** **
	Proportional Distance	-0.688	0.114	-6.030	**<0.001*** **
	Prop. Distance:Grazed	-0.246	0.154	-1.600	0.109
	Prop. Distance: Vegetated	-0.364	0.153	-2.380	**0.018***
10	Intercept	1.686	0.244	6.920	
	Grazed Vegetation	-1.453	0.179	-8.120	**<0.001*** **
	Full Vegetation	-1.648	0.179	-9.200	**<0.001*** **
	Proportional Distance	-0.064	0.119	-0.540	0.589
	Prop. Distance:Grazed	-0.354	0.159	-2.230	**0.026***
	Prop. Distance: Vegetated	-0.437	0.159	-2.740	**0.006****
100	Intercept	3.744	0.248	15.090	
	Grazed Vegetation	0.043	0.117	0.360	0.716
	Full Vegetation	-3.190	0.192	-16.600	**<0.001*** **
	Proportional Distance	-3.255	0.192	-16.960	**<0.001*** **
	Prop. Distance:Grazed	-0.537	0.160	-3.350	**0.001*** **
	Prop. Distance: Vegetated	-0.508	0.159	-3.190	**0.001*** **

Supplementary Table S9: Vegetation drives progressive reductions in channel water depths with increasing distance upstream. Statistical model summary of the effects of vegetation state, proportional distance upstream and their interaction on flood depth within 1km long estuary "zones".

Event	Predictor	Estimate	S.E.	Z-value	P
1	Intercept	0.86	0.20	4.36	
	Grazed Vegetation	-0.27	0.07	-3.82	**<0.001*** **
	Full Vegetation	-0.34	0.07	-4.83	**<0.001*** **
	Proportional Distance	-8.11	1.01	-8.01	**<0.001*** **
	Prop. Distance:Grazed	-4.30	1.42	-3.03	**0.002****
	Prop. Distance: Vegetated	-8.28	1.41	-5.87	**<0.001*** **
10	Intercept	1.30	0.26	4.99	
	Grazed Vegetation	-0.24	0.08	-2.84	**0.005****
	Full Vegetation	-0.30	0.08	-3.59	**<0.001*** **
	Proportional Distance	-9.76	1.24	-7.55	**<0.001*** **
	Prop. Distance:Grazed	-4.42	1.71	-2.58	**0.010***
	Prop. Distance: Vegetated	-5.05	1.71	-2.96	**0.003****
100	Intercept	3.49	0.21	16.62	
	Grazed Vegetation	-1.36	0.14	-10.09	**<0.001*** **
	Full Vegetation	-1.25	0.13	-9.38	**<0.001*** **
	Proportional Distance	3.36	1.79	1.88	0.060
	Prop. Distance:Grazed	-19.57	2.51	-7.80	**<0.001*** **
	Prop. Distance: Vegetated	-19.66	2.53	-7.79	**<0.001*** **

Supplementary Table S10: Vegetation drives progressive reductions in flood extent with increasing distance upstream. Statistical model summary of the effects of vegetation state, proportional distance upstream and their interaction on flood extent within 1km long estuary "zones".

Event	Predictor	Estimate	S.E.	Z-value	P
1	Intercept	-0.14	0.17	-0.84	
	Grazed Vegetation	-0.47	0.13	-3.63	**<0.001*** **
	Full Vegetation	-0.61	0.13	-4.71	**<0.001*** **
	Proportional Distance	2.74	1.81	1.52	0.129
	Prop. Distance:Grazed	-6.20	2.59	-2.39	**0.017***
	Prop. Distance: Vegetated	-5.93	2.58	-2.30	**0.022***
10	Intercept	1.03	0.15	6.81	
	Grazed Vegetation	-0.68	0.14	-4.69	**<0.001*** **
	Full Vegetation	-0.75	0.14	-5.22	**<0.001*** **
	Proportional Distance	-1.71	2.05	-0.83	0.400
	Prop. Distance:Grazed	-4.52	2.91	-1.56	0.120
	Prop. Distance: Vegetated	-5.96	2.90	-2.05	**0.040***
100	Intercept	1.67	0.14	11.61	
	Grazed Vegetation	-0.96	0.14	-6.68	**<0.001*** **
	Full Vegetation	-0.85	0.14	-5.90	**<0.001*** **
	Proportional Distance	1.78	1.95	0.91	0.361
	Prop. Distance:Grazed	-6.33	2.87	-2.21	**0.027***
	Prop. Distance: Vegetated	-5.99	2.88	-2.08	**0.038***

Supplementary Figure S2: Estuary-scale decreases in flood current velocity in upstream areas are driven by marsh vegetation. Differences in water flood current between unvegetated and vegetated scenarios for a 1 in 100 Storm, Green colours (positive values) indicate enhancement of current velocity due to vegetation, and warmer yellows to reds (negative values) indicate flood current velocity reduction caused by vegetation. Results presented for the Neath (**A**), Loughor (**B**), Three Rivers Complex (Taf, Towy, Gwendraeth) (**C**), Mawddach (**D**), Glaslyn (**E**) and Dee (**F**) estuaries. In units of meters per second (ms)

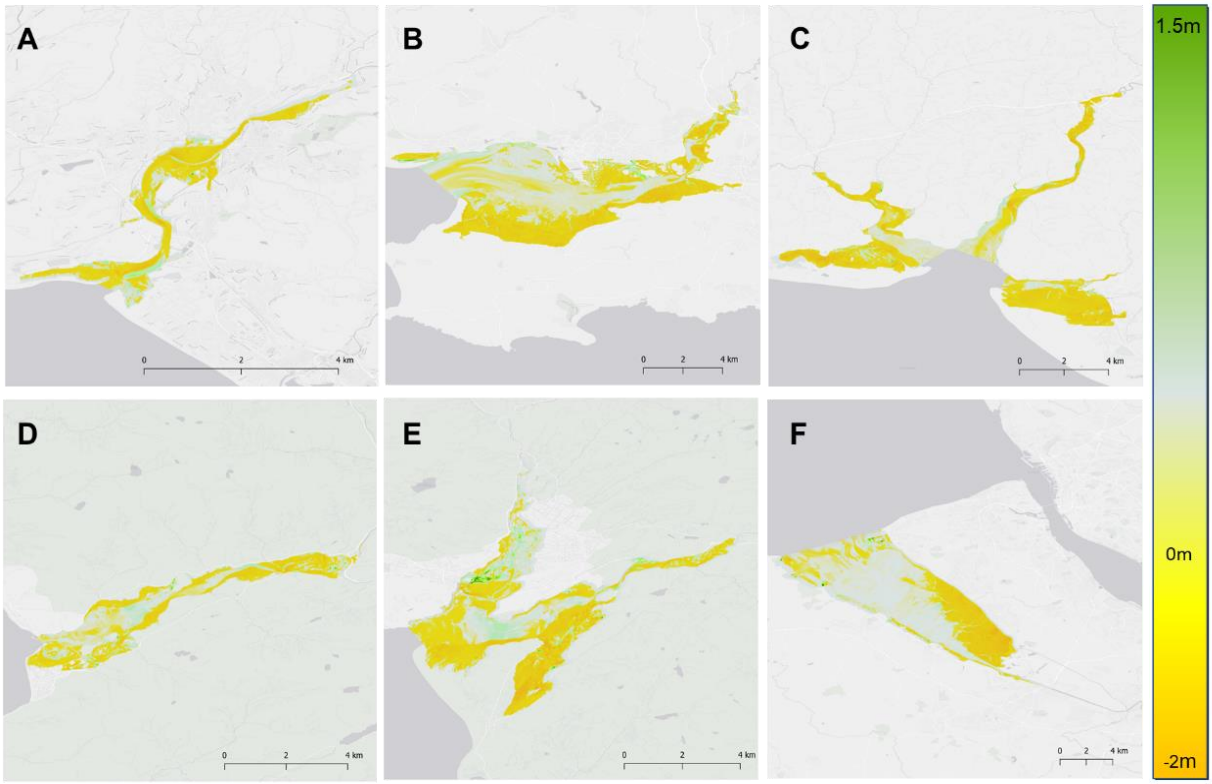

Supplementary Table S11: Marsh vegetation is less effective at reducing up-stream surge in larger estuaries. Statistical model summary of the effects of Estuary Size (km²), marsh proportion and storm intensity on proportional reductions of surge at upstream tidal limits.

Predictor	Estimate	S.E.	T-value	P
Intercept	-0.069	0.454	-0.151	
Estuary Size	-0.548	0.111	-4.940	**<0.001*** **
Marsh Proportion	0.013	0.007	1.859	0.080
Storm	0.001	0.005	0.170	0.867
Estuary Size:Storm	-0.001	0.002	-0.679	0.506

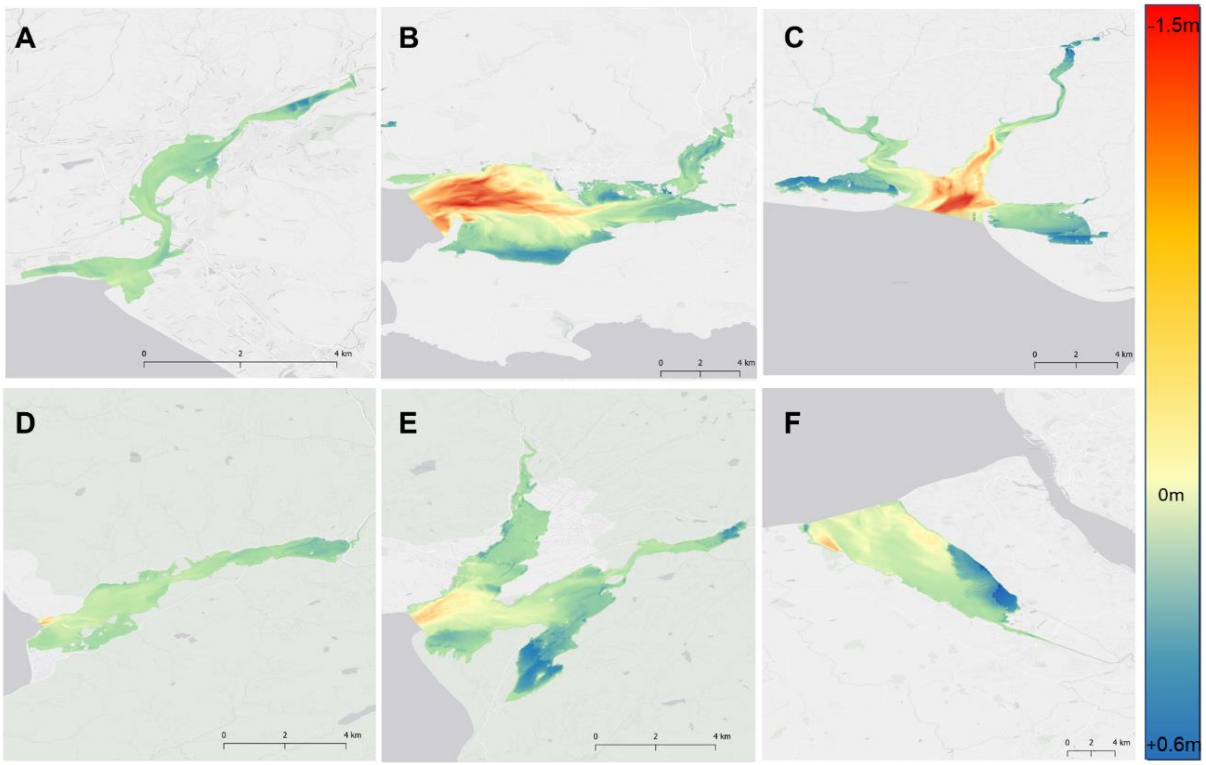

Supplementary Figure S3: Wave heights are amplified by vegetation close to estuary mouths, but decay quickly due to vegetation drag in upstream areas. Differences in wave height between unvegetated and vegetated scenarios for a 1 in 100 Storm, Warm colours (negative values) indicate enhancement of wave height due to vegetation, and cooler blues (positive values) indicate wave height reduction caused by vegetation. Results presented for the Neath (**A**), Loughor (**B**), Three Rivers Complex (Taf, Towy, Gwendraeth) (**C**), Mawddach (**D**), Glaslyn (**E**) and Dee (**F**) estuaries. In units of meters (m).

Supplementary Table S12: Marsh vegetation attenuates upstream wave propagation, and strengthens with the proportional distance upstream. Statistical model summary of the effects of vegetation state, proportional distance upstream and their interaction on wave height within 1km long estuary "zones".

Event	Predictor	Estimate	S.E.	Z-value	P
1	Intercept	0.03	0.19	0.15	
	Grazed Vegetation	-0.21	0.11	-1.96	**0.04***
	Full Vegetation	-0.45	0.11	-4.09	**<0.001*****
	Proportional Distance	-13.91	1.57	-8.85	**<0.001*****
	Prop. Distance:Grazed	-3.83	2.21	-1.73	0.08
	Prop. Distance: Vegetated	-7.61	2.23	-3.41	**<0.001*****
10	Intercept	-0.210	0.308	-0.680	
	Grazed Vegetation	-0.308	0.213	-1.440	0.149
	Full Vegetation	-0.334	0.210	-1.590	0.113
	Proportional Distance	-0.520	0.111	-4.690	**<0.001*****
	Prop. Distance:Grazed	-0.071	0.155	-0.450	0.650
	Prop. Distance: Vegetated	-0.395	0.159	-2.480	**0.013***
100	Intercept	2.21	0.20	11.25	
	Grazed Vegetation	-1.22	0.14	-8.81	**<0.001*****
	Full Vegetation	-0.891	0.14	-6.49	**<0.001*****
	Proportional Distance	7.88	1.95	4.05	**<0.001*****
	Prop. Distance:Grazed	-22.09	2.80	-7.90	**<0.001*****
	Prop. Distance: Vegetated	-33.29	2.80	-11.89	**<0.001*****

Supplementary Table S13: Marsh vegetation locally attenuates waves traveling over marsh platforms, and wider marshes were the most effective and consistent. Statistical model summary of the effects of vegetation state, marsh width, marsh slope, overlying water depth, initial wave height at marsh-estuary boundary and distance upstream on wave transformation over marshes.

Event	Predictor	Estimate	S.E.	Z-value	P
1	Intercept	-2.470	0.597	-4.140	
	Marsh Width	0.562	0.090	6.240	**<0.001*** **
	Grazed	-0.001	0.495	0.000	0.999
	Vegetated	0.734	0.507	1.450	0.147
	Marsh Width:Grazed	0.029	0.089	0.330	0.745
	Marsh Width:Vegetated	-0.038	0.091	-0.420	0.678
	Slope	23.900	4.270	5.590	**<0.001*** **
	Depth Over Marsh	-0.371	0.114	-3.260	**0.001*** **
	Distance from Mouth	0.000	0.000	0.190	0.846
	Initial Wave Height	-0.204	0.349	-0.580	0.559
10	Intercept	-0.813	0.562	-1.450	
	Marsh Width	0.149	0.079	1.900	0.058
	Grazed	-1.310	0.426	-3.080	**0.002** **
	Vegetated	-1.350	0.432	-3.110	**0.002** **
	Marsh Width:Grazed	0.269	0.076	3.550	**<0.001*** **
	Marsh Width:Vegetated	0.309	0.077	4.010	**<0.001*** **
	Slope	17.200	3.710	4.650	**<0.001*** **
	Depth Over Marsh	-0.550	0.084	-6.570	**<0.001*** **
	Distance from Mouth	0.000	0.000	1.780	0.075
	Initial Wave Height	0.751	0.308	2.440	**0.015***
100	Intercept	-2.450	0.598	-4.100	
	Marsh Width	0.413	0.087	4.750	**<0.001*** **
	Grazed	-0.674	0.437	-1.540	0.123
	Vegetated	-0.518	0.436	-1.190	0.234
	Marsh Width:Grazed	0.159	0.079	2.020	**0.044***
	Marsh Width:Vegetated	0.167	0.078	2.130	**0.033***
	Slope	26.700	6.210	4.300	**<0.001*** **
	Depth Over Marsh	-0.385	0.106	-3.630	**<0.001*** **
	Distance from Mouth	0.000	0.000	-0.890	0.372
	Initial Wave Height	0.913	0.294	3.110	**0.002** **

Supplementary Table S14: Marsh vegetation locally attenuates flood water traveling over marsh platforms, and wider marshes were the most effective and consistent. Statistical model summary of the effects of vegetation state, marsh width, marsh slope, overlying water depth, initial wave height at marsh-estuary boundary and distance upstream on flood water depths at terrestrial boundaries.

Event	Predictor	Estimate	S.E.	Z-value	P
1	Intercept	-1.100	0.547	-2.010	
	Marsh Width	0.423	0.084	5.030	**<0.001*** **
	Grazed	-0.372	0.464	-0.800	0.423
	Vegetated	-0.763	0.463	-1.650	0.099
	Marsh Width:Grazed	0.096	0.084	1.140	0.253
	Marsh Width:Vegetated	0.184	0.083	2.200	**0.027***
	Slope	31.700	4.260	7.440	**<0.001*** **
	Depth Over Marsh	-0.609	0.100	-6.090	**<0.001*** **
	Distance from Mouth	0.000	0.000	0.640	0.524
	Initial Wave Height	-0.243	0.306	-0.800	0.426
10	Intercept	-0.340	0.550	-0.620	
	Marsh Width	0.195	0.076	2.570	**0.010***
	Grazed	-1.060	0.396	-2.680	**0.007****
	Vegetated	-1.000	0.398	-2.520	**0.012***
	Marsh Width:Grazed	0.231	0.071	3.280	**0.001*** **
	Marsh Width:Vegetated	0.242	0.071	3.430	**0.001*** **
	Slope	24.500	4.140	5.920	**<0.001*** **
	Depth Over Marsh	-0.519	0.078	-6.660	**<0.001*** **
	Distance from Mouth	0.000	0.000	-0.560	0.576
	Initial Wave Height	0.196	0.289	0.680	0.497
100	Intercept	-1.790	0.481	-3.720	
	Marsh Width	0.403	0.068	5.940	**<0.001*** **
	Grazed	-0.880	0.368	-2.390	**0.017***
	Vegetated	-1.300	0.368	-3.530	**<0.001*** **
	Marsh Width:Grazed	0.185	0.066	2.800	**0.005****
	Marsh Width:Vegetated	0.267	0.066	4.050	**<0.001*** **
	Slope	59.800	5.170	11.560	**<0.001*** **
	Depth Over Marsh	-0.532	0.082	-6.500	**<0.001*** **
	Distance from Mouth	0.000	0.000	-0.360	0.716
	Initial Wave Height	0.214	0.219	0.980	0.329

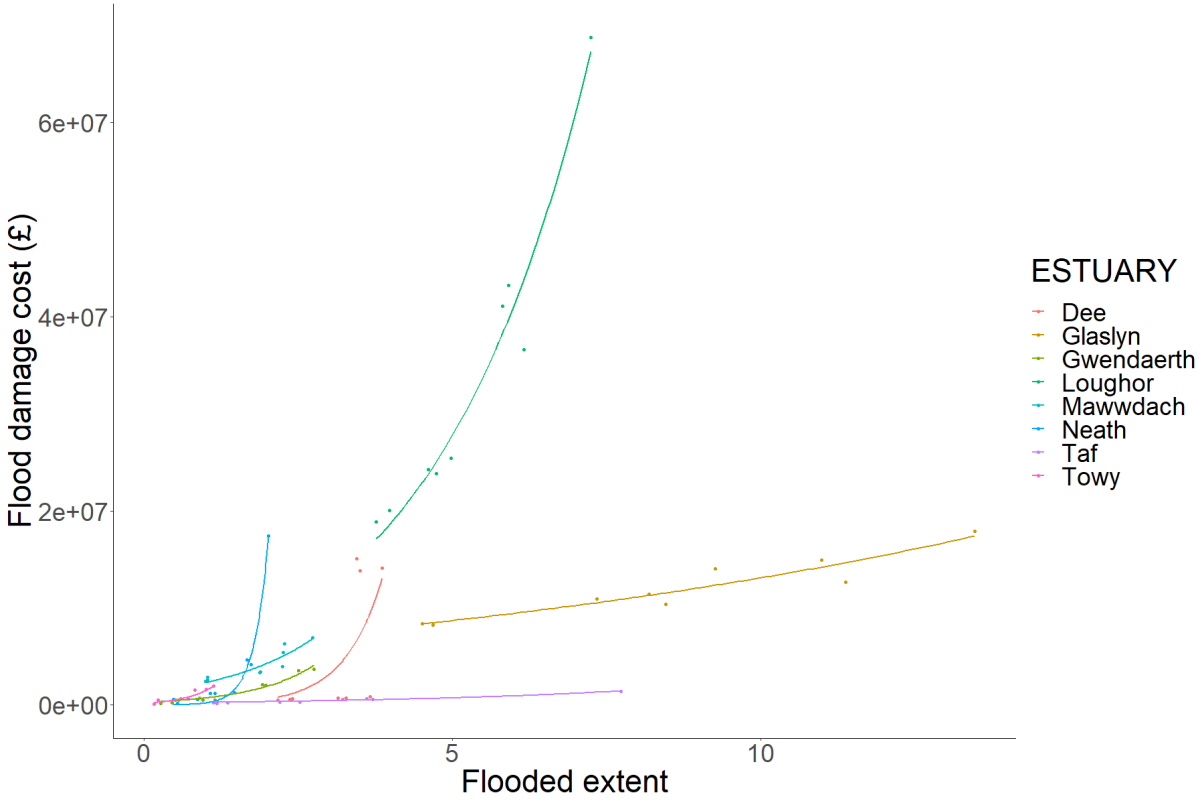

Supplementary Figure S4: General non-linear relationships between flood area and flood damage cost for estuaries in the this study. Most estuaries display exponential increases in cost with increasing flood extent, except for the Taf and Glaslyn estuaries in which low lying land is almost exclusively low-value agricultural or common land.

3: Additional Methodological Details

3.1: Hydrodynamic models

In order to investigate the role of saltmarsh vegetation on estuarine hydrodynamics and coastal flooding risk during storm events we created online coupled Delft3D FLOW and WAVE (SWAN Cycle III 41.31) models[29] using 2-dimensional (depth averaged) form of unsteady shallow water equations[29] across eight case study estuaries (Supplementary Figure S5). Models were constructed using structured grids, gradually refining from 150x50m grids at offshore locations (to ca. 25m below chart datum), to uniform, high resolution 10 x 10m grids throughout the estuary boundaries. To adequately represent the hydrodynamics, we used 0.01 minute calculation timesteps, and 15 minute output intervals to capture tide and storm surge peaks as they progressed up-stream. Following modelling, we combined data from multiple output intervals, between the water level peak at the estuary mouth, to the water level peak at the Limit of Tidal Intrusion (LTI), to create maximum extent, depth, current and wave maps using the mosaic function in QGIS 3.10.2[30].

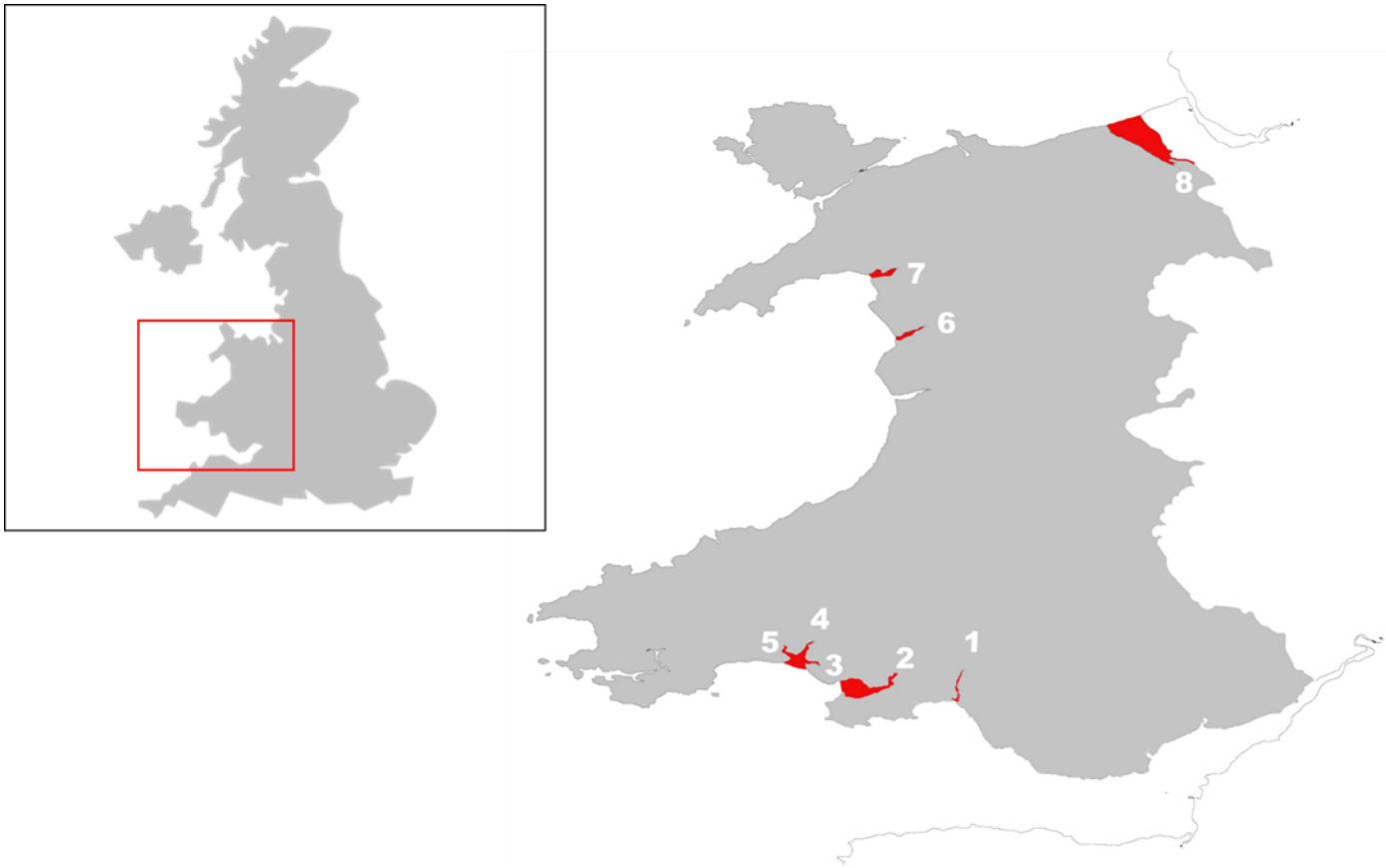

Supplementary Figure S5: Map of the 8 selected estuaries within Wales, UK used in this study: 1) Neath, 2) Loughor, 3) Gwendraeth, 4) Towy, 5) Taf, 6) Mawddach, 7) Glaslyn & 8) Dee

3.2: Inputs

To Accurately characterise the hydrodynamics of the estuaries, the computational models were calibrated and populated with validated observed and modelled data for bathymetries, tides, surge profiles, waves river flows and wind.

3.2.1 Bathymetries

To accurately represent the hydrodynamics in the estuaries and coastal regions, topobathymetries for each estuary and offshore model extent were created using raster EMODNET bathymetries (https://www.emodnet.eu/bathymetry) for open water areas, and high resolution (1m) LiDAR DTM data (available from http://lle.gov.wales) for inshore, estuarine and terrestrial areas. An additional sonographic survey (heave/surge compensated Lowrance Structure Scan 3D transducer) was also undertaken using a ridged inflatable vessel

in the Taf Estuary, where LiDAR data quality and coverage was poor in estuary channel areas. Outputs were converted, scaled and mosaiced using base routines using QGIS 3.10.2[30] to create topobathymetries matching the grid resolution of the hydrodynamic models.

3.2.2: Boundary Conditions

3.2.2.1: Tidal conditions

Harmonic tidal predictions were determined for each boundary grid cell using the TPXO 8.0[31] tidal prediction model using the DelftDashboard Tool Suite (TU Delft). Tidal models were then created using the harmonics derived from TPXO 8.0 using Delft3D-FLOW, producing a 1-year tidal model for each estuary. From these models, the largest tide was selected, and the resulting time-varying boundary water levels were used to specify the boundary conditions, along with surge profiles (below in 3.2.2.2), for the coupled FLOW-WAVE storm models.

3.2.2.2: Storm conditions:

Statistically significant water level variations during storms were determined following the method given in McMillan et al.[32] For each estuary, we used storm surge level data supplied by the National Tide and Sea Level Facility of the UK (NTSLF) using the skew surge joint probability method (SSJPM), and tidal predictions (see 3.2.2.1) to calculate total water levels for the storm scenarios, following the methodology of Bennett et al.[33]. In this study, we assumed that storm peaks coincides with high tide, and that the maximum surge occurs at the peak of the storm, representing worst-case storm event scenarios.

Additionally to tidal and storm surges, we simulated the effects of waves and wave set-up. We used the Centre for Environment Fisheries and Aquaculture Science (CEFAS) Wavenet database to parameterise offshore waves, using hindcast output points closest to each estuary modelled. From this data, storms occurring between 1980-2018 were isolated following the method described in Bennett et al.[33], and based on the storm definitions provided by Dissanayake et al.[34]. Storms were defined by a threshold storm wave height of 2.5 m, based on the U.K. Channel Coastal Observatory (CCO) guidance for defining storm thresholds[35]. The Generalised Pareto Distribution (GPD), utilising the R package ismev[36], was then used to

1007 determine significant storm wave heights corresponding to 1 in 1-, 1 in 10-, and 1 in 100-year
1008 return periods. The wave models for each estuary were then populated with the derived
1009 average significant storm wave height (W_{avg}), maximum storm wave period (T_{max}) and the
1010 average predominant wave direction for all individual storm events (Wd_{avg}) for each storm
1011 scenario at the offshore model boundary.

1012 We also considered wind effects on wave propagation and internal generation of waves in the
1013 estuaries. We identified and used hourly outputs of wind speed and direction, between
1014 January 1977 and January 2018, from weather stations close to each estuary from the U.K.
1015 Meteorological Office weather stations network as part of the MIDAS dataset
1016 (https://catalogue.ceda.ac.uk/). Similarly to the analysis of storm wave data, storm wind data
1017 was filtered to include events where wind speed was >20m/s, and the GPD was fitted to the
1018 wind data to give average wind speed for each storm return-level (Wi_{avg}). The predominant
1019 wind direction was also then determined from the average observed wind data during storm
1020 conditions (Wi_{d}).

1021 The storm wave and wind conditions were then used to generate time-varying storm profiles
1022 using three-point spline curves, which closely represented observed storm profiles. In this,
1023 storms began when incident wave height and wind speed exceeded the pre-selected threshold
1024 wave height and wind speed, and ceased when wave height and wind speed became smaller
1025 than the threshold. In our scenarios, storm peaks occurred halfway between the beginning
1026 and the end of storm, creating a symmetric storm profile, and giving an average storm duration
1027 of 75 hours across the estuaries. The time-varying storm conditions were then passed to the
1028 DELFT-3D WAVE and FLOW modules to commence storm hydrodynamic modelling.

1029 **3.2.2.3: River inputs:**

1030 Inspection of weather records for Wales (Met Office) indicated that the largest storms with
1031 high wind speeds often experienced substantial rainfall, but were not generally coupled to the
1032 highest rainfall totals (personal observation). As a result, we selected river flow records for
1033 each river at the Q_5 exceedance level, where discharged water volume is only exceeded on

5% of days within an average year, rather than Q_{max} maximum recorded water discharge. Data for river discharges is available through the National River Flow Archive Wales (Centre for Ecology and Hydrology [CEH], available at nrfa.ceh.ac.uk). River flows were specified at each major river channel up-stream boundary as a continuous flow in the Delft3D models.

3.2.3: Vegetation

Salt marsh vegetation parameters and extents were provided to the FLOW and WAVE modules to understand the role that vegetation plays in preventing coastal flooding in estuaries. Marsh shapefiles provided by Natural Resources Wales (available at: http://lle.gov.wales/catalogue/item/SaltmarshExtents) were used to populate the extents of marsh area within each estuary, and we undertook field campaigns to map plant distributions and quantify key plant properties within each estuary, which were then used to calculate community weighted means (CWM) for key plant traits used as vegetation inputs in this study (Supplementary Table S14). March vegetative communities tended to be dominated by mixtures of *Atriplex portulacoides*, *Spartina anglica*, and mixed communities of *Festuca rubra*, *Tripolium pannonicum*, *Suaeda maritima* and *Puccinellia maritima*.

Supplementary Table S15: Vegetation Parameters derived from field surveys, used to populate vegetation models.

Mean Plant Density (Stems per m²) (n_v)	Mean Vegetation Height (m) (h_v)	Mean Stem Thickness (base) (mm)	Mean Stem Thickness (tip) (mm)	Plant drag coefficient (C_d)
2275	0.33	3.3	1.8	1

In this study we modelled Saltmarsh vegetation using simplified rigid cylinders that are parameterized by plant height h_v, plant density n_v, and stem diameter which reduces towards the end of stems which were derived from CWM from the survey data.

We modelled the drag force induced by rigid cylindrical saltmarsh vegetation on currents as a sink term in the momentum equations (Equation 1)

$$\vec{F} = \frac{1}{2}\rho C_D b_v n_v |\vec{u}|\vec{u}.$$

where F is the drag force produced by vegetation per unit volume in N/m3, ρ is the density of the fluid in kg/m^3, u is the local flow velocity in m/s., and C_D is a dimensionless drag coefficient. Owing to the inability to measure drag (C_d) in the field, a priori, we assumed $C_d = 1$ based on previous experimental studies with stiff cylinders in unidirectional flow and under similar wave conditions[37,38], and has been applied successfully to previous studies on saltmarsh vegetation.

In addition to modification of flow, we also looked at the role of vegetation on wave energy using the same rigid cylinder approach. Saltmarsh vegetation dampens waves owing to the work done by the drag force (Equation (2)) on plants stems, implemented in Delft3D WAVE via Equation 2.

$$\frac{\partial E c_g}{\partial x} = < \int_{-h}^{-h+h_v} \vec{F}\vec{u} dz >,$$

Where $E = \frac{1}{8}\rho g H^2$ is the wave energy density in N/m, c_g is the group velocity in m/s, h is the water depth in meters and h_v is the vegetation height in meters. The horizontal axis x is in the direction of wave propagation, z is the vertical axis in the water column and brackets (<)) denote phase-averaging.

3.2.4: Model Validation

To ensure that hydrodynamic models adequately captured the hydrodynamics in estuaries, we tested observed data – centred around large spring tide events - against calibrated models using at a number of locations throughout the estuaries. We used a combination of observed data from river and tidal gauging stations (Natural Resources Wales [NRW] and British Oceanographic Data Centre [BODC]) of known elevation, and deployed atmospherically-corrected water depth loggers (HOBO UL21, in pairs) with elevation determined using a GNSS RTK receiver (Leica Viva GS08), to determine water levels for each location. Modelled water levels - for the prevailing conditions during validation data collection - were compared against the observed data, and model performance metrics (R^2, RMSE) calculated. Due to a lack of existing storm wave data from inshore or estuary locations, wave heights were not directly

validated. However, the spectral wave models (SWAN cycle III 41.31) within our Delft-3D framework have been extensively validated [39–41], and previous studies of wave heights using Delft-3D WAVE with SWAN – including in complex estuarine environments [42–44] and wave-vegetation interactions[2] – have demonstrated the reliability and accuracy of the model predictions across a range of comparable environments. Furthermore, sampling of water levels at both the Neath Castle and Laugharne North stations (denoted by an asterix (*) in Supplementary Table S16) coincided with minor storms, and water levels included wave-set up effects which were included in validation models, allowing for limited indirect validation of wave models. Overall, models performed well for each tested location (Supplementary Figure S6, Supplementary Table S15), particularly around the crucial high-water peaks, and sufficiently predicted water levels.

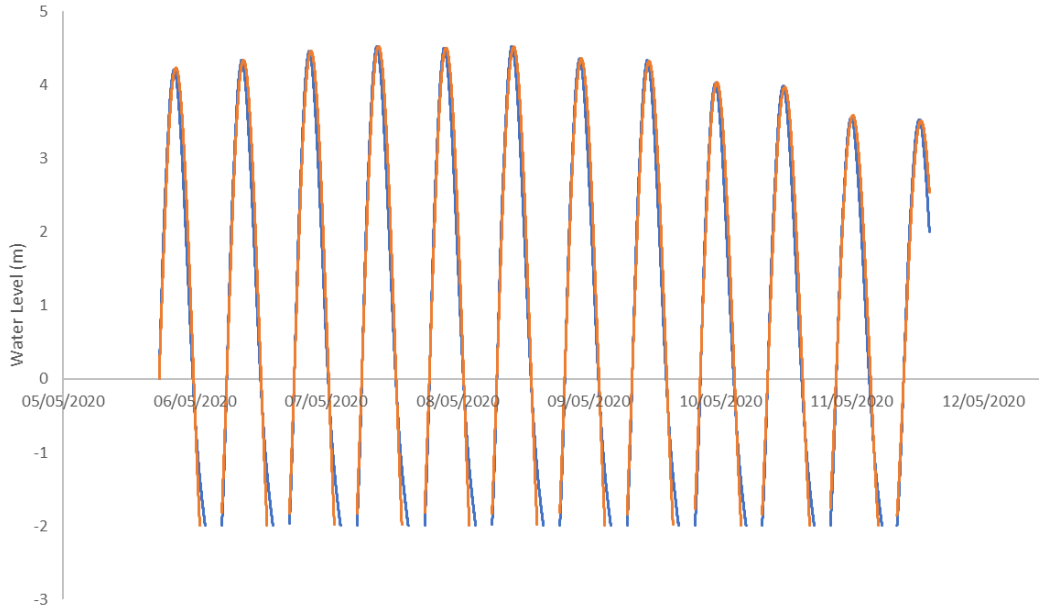

Supplementary Figure S6: Model validation of water levels at Burry Port, Loughor estuary show good agreement with measured water levels (R^2=0.97, RMSE=0.27m). Modelled peak high water values vary by <0.05m compared with the observed water levels. Orange lines represent measured values, and blue represent modelled values. Missing values during low tide are due to drying out of the location.

Supplementary Table S16: Modelled water levels show good agreement with observed values at monitoring points in the estuaries, and are suitably well fitting to allow assessment of the role of marsh vegetation in mitigating storm flood impacts. For each location the distance upstream is provided along with the observation measure, model agreement parameters (R^2, RMSE), and the difference in water level between observed and predicted at peak high tide (positive values indicate modelled > observed, and negative modelled<observed).

Estuary (location)	Distance Upstream	Measure	R^2	RMSE (m)	Peak High Water Level Difference (m)
Neath Castle*	6km	Depth Logger (atm corr)	0.984	0.101	0.04
Loughor (Burry Port)	4km	Depth Logger (atm corr)	0.974	0.272	-0.03
Loughor (Llanelli docks)	7km	Tidal Gauge (NRW)	0.954	0.295	0.06
Three Rivers: Taf (Laugharne South)	3km	Depth Logger (atm corr)	0.789	0.163	0.05
Three Rivers: Taf (Laugharne North)*	6km	Depth Logger (atm corr)	0.998	0.069	-0.05
Mawddach (Barmouth RW Bridge)	1km	Tidal Gauge (BODC)	0.978	0.234	0.07
Dee (Hilbre Island)	2km	Depth Logger (atm corr)	0.996	0.101	0.05
Dee (Connah's Quay)	22km	Depth Logger (atm corr)	0.987	0.210	-0.12

3.3: Economic analysis

To quantify the economic value that saltmarshes deliver through mitigating floods, we apply methods used by the UK government to appraise investments in flood-protection infrastructure[45,46]. We compared the flood damages experienced in each estuary when marshes have no vegetation to those with full or grazed vegetation. Our calculations aggregated flood damage estimates for residential, commercial, industrial and agricultural properties, as well as to public buildings and water and electricity utility installations using flood cost estimates from the 2018 update of the Multi-Coloured Manual (MCM)[46]. For each estuary under each scenario, we overlaid the gridded outputs from the hydrodynamic modelling with OS Mastermap topography layer. OS MasterMap topography layer is the most detailed topographic map produced by Great Britain's national mapping agency, the Ordnance Survey

(OS) (Ordnance Survey 2020). From OS Mastermap we were able to identify each property that intersected a flooded grid cell and attribute each with a flood depth. Where a property spanned more than one grid cell, that property was associated with the maximum flood depth. We restricted attention to buildings with a footprint over 25m^2, of which some 2,331 were in flood-effected areas across the study estuaries. No comprehensive secondary dataset was available to establish the characteristics of those properties. Accordingly, each building was inspected manually using both satellite and Google Streetview imagery[47]. That inspection allowed us to establish the type (i.e. terraced, semi-detached, detached, bungalows and flats) and age of each residential property (i.e. pre-1919, 1919-44, 1945-64, 1965-74, 1975-85 and post-1985). In addition, small area data (Output Area) from the 2011 UK Census[48] was used to establish the socioeconomic grade characterising a property's neighbourhood. Ultimately, a flooded residential building was characterised by type, age, socioeconomic band and flood depth. Using that building-specific characterisation, estimates of short-duration saltwater inundation damages to building fabric, household inventory and domestic clean-up were taken from MCM cost tables[46] (full cost tables are available at https://www.mcm-online.co.uk/handbook). Where a property spanned the boundary of flood extent, only a proportion of the damage cost was used in our calculations, where that proportion was equal to the percentage of the property in the flooded area.

Non-residential buildings were first attributed a detailed characterisation which was later amalgamated into nine-category classification; public buildings (including schools, doctor's surgeries. hospitals and community centres), industrial buildings (including factories, workshops, agricultural barns and water treatment works), retail properties (including shops, supermarkets, petrol stations, vehicle repair garages, pubs, cafés and restaurants), offices, warehouses, leisure facilities (including hotels, theatres and cinemas), electricity substations, sports centres and sports stadia. Category-specific damage costs per metre squared for saltwater inundation to the flood depth experienced at each non-residential building were

taken from MCM cost tables[46] (available at https://www.mcm-online.co.uk/handbook) assuming a short duration of inundation but without prior warning of the flood event. The per metre-squared costs were multiplied up by the area of the building footprint experiencing flooding to arrive at the damage cost estimate.

For each estuary the length of motorway, A-road, B-road and minor road inundated in a flood event were identified from the OS Integrated Transport Network data layer. Taking an average over the five years from 2014 to 2018, daily traffic flows by vehicle type (specifically; cars, public service vehicles, light goods vehicles, and heavy goods vehicles) for each category of road in each estuary's local authority region (specifically; Flintshire, Gwynedd, Carmarthenshire and Neath/Port Talbot) were sourced from Department for Transport road traffic statistics (DfT, 2020). Those daily flows were converted to average hourly flows. To calculate disruption costs from flooding we applied the 'diversion-value method'. Specifically, we assumed that each journey that would otherwise have used the flooded road, would instead be diverted via a longer route. For the sake of simplicity we assumed that diversion to extend the journey by a distance equal to the length of road made impassable by the flood water. Further assuming a standard 12-hour period of flooding for each storm event we calculated the number of journeys by each vehicle type subject to such an extended journey and multiplying up by the length of diversion arrived at estimates of the additional flood-induced journey distances by each vehicle type on each road category. We arrived at our final estimates of travel-disruption costs by multiplying up those estimates by vehicle- and road-specific costs per kilometre of additional travel provided in the MCM cost tables.

Parks and paths used for outdoor recreation impacted by flooding were identified from the Outdoor Recreation Valuation (ORVal) greenspace map[49]. Estimates for the annual recreation value generated by those sites was accessed from the ORVal tool[50]. Losses from disruption of recreation activity were calculated by assuming that the flood event restricted access to those recreation sites for one week. Where a recreation site straddled the flood extent

boundary, recreation costs were adjusted by a quantity equal to the percentage of the site experiencing flooding.

Agriculture land parcels inundated with saltwater in each flood event were identified from Landcover Map 2015[51] and categorised as either grazing pasture or as arable. Damage costs were taken from the MCM cost tables using the simplified aggregate costs from a single annual flood by land use. For pasture costs were estimated at £180 per hectare and those for arable at £501 per hectare[46]

Damage costs for a particular event assuming a particular state of marsh vegetation in an estuary are calculated by adding together the property, utility, road, agriculture and recreation cost estimates for that event. To estimate expected annual damages in each estuary, we construct a flood probability-damage curve. Our damage cost estimates provide three points on that curve relating to the 1 in 1 event, (annual probability of 1) 1 in 10 event (annual probability of 0.1) and the 1 in 100 event (annual probability of 0.01). We make the conservative assumption that flood events with magnitude greater than the 1 in 100 event cause the same damage as the 1 in 100 event. Likewise we assume that flood events with magnitude less than the 1 in 1 event generate no damage costs. We complete the probability-damage curve by linearly interpolating damage costs between the estimated 1 in 1 event, 1 in 10 event and 1 in 100 event costs. The expected annual damages can then be calculated by integrating under the probability-damage curve from 0.01 to 1.

Assuming a 50-year appraisal period we adopt UK government recommended discount rates to calculate the present value of those damage costs[45]. Our estimates of the economic value of maintaining saltmarsh in its natural state is taken to be the reduction in the present value of damage costs that arises from natural vegetation as compared to when that vegetation is grazed or lost.

3.4: Assumptions and Limitations of modelling methodologies:

Hydrodynamic modelling using Delft3D has been validated and performs well for a variety of scenarios[33,39,40,52], but as with any modelling exercise it makes assumptions and approximations of physical processes which may not always capture every nuance of the environment. For instance, our modelling approach used 2-dimensional high resolution (ca. 10 x 10m) depth averaged models which capture large scale processes well, but may miss effects from small features. Features of 10x10m or smaller are not well captured by the model as they are at or below the resolution of the model (Nyquist limit), but may alter local hydrodynamics. These features may also include some small scale, low-crested and single layer coastal defence walls along isolated sections of estuary (see supplementary Figure S7) which were too small to be represented in the models, or on the LiDAR and satellite imagery which were used to identify features, and may have lead to isolated pockets of flooding that would not have occurred in the presence of structures.

Estuary and offshore topobathymetries were constructed using a combination of EMODNET and LiDAR raster images. However, in some estuaries (notably the Taf), LiDAR data has been created from composites from different time points, leading to stepped edges where either bed morphology has changed, or fly-overs have been conducted at different points in the tide, leading to localised inconsistencies in the bathymetries. We corrected these by manually adjusting points where this occurred using the QuickIN utility in Delft-3D to approximate bathymetric profiles, but these smoothed approximations my exclude conspicuous features on the bed. It is also important to note that the LiDAR data was often more than five years old, and may not reflect current bathymetries, especially in dynamic estuaries. Instead, they provide an approximated “snap-shot” which we can use to evaluate the role of vegetation, rather than current flood risk, and outputs should not be used to infer flood potential in any of the case-study estuaries.

Supplementary Figure S7: Low-crested (approx.. 1m), narrow coastal defence walls such as this one between Loughor and Llanelli may be absent within the model domains due to their small size.

Vegetation also introduces additional element of uncertainty. Currently, the vegetation implementation in coupled Delft3D-WAVE (SWAN Cycle III 41.31) models only allows a single vegetation type to be specified, with regards to height, diameter and drag, whereas marshes are complex mosaics of different species which are likely to vary in their hydrodynamic properties. To overcome this, we used community weighted means of species traits from vegetation surveys to capture estuary level marsh properties. While this should give a good representation of the vegetation under most circumstances, the contributions of some marshes may be over- or under-estimated due to deviation of overall marsh characteristics from the mean values. For example, some marshes may be dominated by tall, ridged species such as Spartina spp. and Phragmites spp., whereas others may be dominated by low and flexible Festuca spp.

Vegetation in our model also uses ridged cylinders to represent the plants. While rigid-cylinder models of vegetation currently are the best method for the approximation of vegetation effects, they may not fully capture hydrodynamic effects for more flexible species, and could overestimate hydrodynamic drag as flexible vegetation can deform due to water currents[38]. Instead we used conservative drag coefficients for the vegetation (C*d*=1) to reduce the risk of overestimation of marsh effects on hydrodynamics and flood potential, which could underestimate the contribution of marsh vegetation communities in our models, and our predictions should as such be seen as conservative.

References:

1. Wamsley, T. V., Cialone, M. A., Smith, J. M., Atkinson, J. H. & Rosati, J. D. The potential of wetlands in reducing storm surge. *Ocean Eng.* **37**, 59–68 (2010).
2. Meijer, M. C. Wave attenuation over salt marsh vegetation. A numerical implementation of vegetation in SWAN. (2005).
3. Stark, J., Plancke, Y., Ides, S., Meire, P. & Temmerman, S. Coastal flood protection by a combined nature-based and engineering approach: Modeling the effects of marsh geometry and surrounding dikes. *Estuar. Coast. Shelf Sci.* **175**, 34–45 (2016).
4. van Loon-Steensma, J. M., Hu, Z. & Slim, P. A. Modelled Impact of Vegetation Heterogeneity and Salt-Marsh Zonation on Wave Damping. *J. Coast. Res.* **32**, 241–252 (2016).
5. Loder, N. M., Irish, J. L., Cialone, M. A. & Wamsley, T. V. Sensitivity of hurricane surge to morphological parameters of coastal wetlands. *Estuar. Coast. Shelf Sci.* **84**, 625–636 (2009).
6. Temmerman, S., De Vries, M. B. & Bouma, T. J. Coastal marsh die-off and reduced attenuation of coastal floods: A model analysis. *Glob. Planet. Change* **92–93**, 267–274 (2012).
7. Hu, K., Chen, Q. & Wang, H. A numerical study of vegetation impact on reducing storm surge by wetlands in a semi-enclosed estuary. *Coast. Eng.* **95**, 66–76 (2015).
8. Vuik, V., Jonkman, S. N., Borsje, B. W. & Suzuki, T. Nature-based flood protection: The efficiency of vegetated foreshores for reducing wave loads on coastal dikes. *Coast. Eng.* **116**, 42–56 (2016).

9. Haddad, J., Lawler, S. & Ferreira, C. M. Assessing the relevance of wetlands for storm surge protection: a coupled hydrodynamic and geospatial framework. *Nat. Hazards* **80**, 839–861 (2016).
10. Smolders, S., Plancke, Y., Ides, S., Meire, P. & Temmerman, S. Role of intertidal wetlands for tidal and storm tide attenuation along a confined estuary: a model study. *Nat. Hazards Earth Syst. Sci. Discuss.* **3**, (2015).
11. Barbier, E. B., Georgiou, I. Y., Enchelmeyer, B. & Reed, D. J. The Value of Wetlands in Protecting Southeast Louisiana from Hurricane Storm Surges. *PLOS ONE* **8**, e58715 (2013).
12. Narayan, S. *et al.* The Value of Coastal Wetlands for Flood Damage Reduction in the Northeastern USA. *Sci. Rep.* **7**, 9463 (2017).
13. Stark, J., Oyen, T. V., Meire, P. & Temmerman, S. Observations of tidal and storm surge attenuation in a large tidal marsh. *Limnol. Oceanogr.* **60**, 1371–1381 (2015).
14. Yang, S. L., Shi, B. W., Bouma, T. J., Ysebaert, T. & Luo, X. X. Wave Attenuation at a Salt Marsh Margin: A Case Study of an Exposed Coast on the Yangtze Estuary. *Estuaries Coasts* **35**, 169–182 (2012).
15. Ysebaert, T. *et al.* Wave attenuation by two contrasting ecosystem engineering salt marsh macrophytes in the intertidal pioneer zone. *Wetlands* **31**, 1043–1054 (2011).
16. Paquier, A.-E., Haddad, J., Lawler, S. & Ferreira, C. M. Quantification of the Attenuation of Storm Surge Components by a Coastal Wetland of the US Mid Atlantic. *Estuaries Coasts* **40**, 930–946 (2017).
17. Foster-Martinez, M. R., Lacy, J. R., Ferner, M. C. & Variano, E. A. Wave attenuation across a tidal marsh in San Francisco Bay. *Coast. Eng.* **136**, 26–40 (2018).
18. Jadhav, R. & Chen, Q. Field investigation of wave dissipation over salt marsh vegetation during tropical cyclone. *Coast. Eng. Proc.* **1**, 41 (2012).
19. Zhang, X., Lin, P., Gong, Z., Li, B. & Chen, X. Wave Attenuation by Spartina alterniflora under Macro-Tidal and Storm Surge Conditions. *Wetlands* (2020) doi:10.1007/s13157-020-01346-w.

20. Möller, I., Spencer, T., French, J. R., Leggett, D. J. & Dixon, M. Wave Transformation Over Salt Marshes: A Field and Numerical Modelling Study from North Norfolk, England. *Estuar. Coast. Shelf Sci.* **49**, 411–426 (1999).
21. Knutson, P. L., Brochu, R. A., Seelig, W. N. & Inskeep, M. Wave damping inSpartina alterniflora marshes. *Wetlands* **2**, 87–104 (1982).
22. Möller, I. Quantifying saltmarsh vegetation and its effect on wave height dissipation: Results from a UK East coast saltmarsh. *Estuar. Coast. Shelf Sci.* **69**, 337–351 (2006).
23. Möller, I. & Spencer, T. Wave dissipation over macro-tidal saltmarshes: Effects of marsh edge typology and vegetation change. *J. Coast. Res.* 506–521 (2002) doi:10.2112/1551-5036-36.sp1.506.
24. Cooper, N. J. Wave Dissipation Across Intertidal Surfaces in the Wash Tidal Inlet, Eastern England. *J. Coast. Res.* **21**, 28–40 (2005).
25. Morgan, P. A., Burdick, D. M. & Short, F. T. The Functions and Values of Fringing Salt Marshes in Northern New England, USA. *Estuaries Coasts* **32**, 483–495 (2009).
26. Möller, I. *et al.* Wave attenuation over coastal salt marshes under storm surge conditions. *Nat. Geosci.* **7**, 727–731 (2014).
27. Beaumont, N. J., Jones, L., Garbutt, A., Hansom, J. D. & Toberman, M. The value of carbon sequestration and storage in coastal habitats. *Estuar. Coast. Shelf Sci.* **137**, 32–40 (2014).
28. King, S. E. & Lester, J. N. The value of salt marsh as a sea defence. *Mar. Pollut. Bull.* **30**, 180–189 (1995).
29. Roelvink, J. A. & Van Banning, G. Design and development of DELFT3D and application to coastal morphodynamics. *Oceanogr. Lit. Rev.* **11**, 925 (1995).
30. Team, Q. D. QGIS geographic information system. *Open Source Geospatial Found. Proj.* (2016).
31. Dushaw, B. D. *et al.* A TOPEX/POSEIDON global tidal model (TPXO. 2) and barotropic tidal currents determined from long-range acoustic transmissions. *Prog. Oceanogr.* **40**, 337–367 (1997).

32. McMillan, A. *et al. Coastal Flood Boundary Conditionsfor UK Mainland and Islands*. (2011).
33. Bennett, W. G., van Veelen, T. J., Fairchild, T. P., Griffin, J. N. & Karunarathna, H. Computational Modelling of the Impacts of Saltmarsh Management Interventions on Hydrodynamics of a Small Macro-Tidal Estuary. *J. Mar. Sci. Eng.* **8**, 373 (2020).
34. Dissanayake, P., Brown, J., Wisse, P. & Karunarathna, H. Comparison of storm cluster vs isolated event impacts on beach/dune morphodynamics. *Estuar. Coast. Shelf Sci.* **164**, 301–312 (2015).
35. Dhoop, T. *Coastal Wave Network Annual Report 2017.* (2018).
36. Coles, S., Bawa, J., Trenner, L. & Dorazio, P. *An introduction to statistical modeling of extreme values*. vol. 208 (Springer, 2001).
37. Tanino, Y. & Nepf, H. M. Laboratory Investigation of Mean Drag in a Random Array of Rigid, Emergent Cylinders. *J. Hydraul. Eng.* **134**, 34–41 (2008).
38. van Veelen, T. J., Fairchild, T. P., Reeve, D. E. & Karunarathna, H. Experimental study on vegetation flexibility as control parameter for wave damping and velocity structure. *Coast. Eng.* **157**, 103648 (2020).
39. Elias, E. P. L., Walstra, D. J. R., Roelvink, J. A., Stive, M. J. F. & Klein, M. D. Hydrodynamic Validation of Delft3D with Field Measurements at Egmond. 2714–2727 (2012) doi:10.1061/40549(276)212.
40. Hsu, Y. L., Dykes, J. D., Allard, R. A. & Kaihatu, J. M. *Evaluation of Delft3D performance in nearshore flows*. (2006).
41. Williams, J. J. & Esteves, L. S. Guidance on Setup, Calibration, and Validation of Hydrodynamic, Wave, and Sediment Models for Shelf Seas and Estuaries. *Adv. Civ. Eng.* **2017**, e5251902 (2017).
42. Elias, E. P. L., Gelfenbaum, G. & Westhuysen, A. J. V. der. Validation of a coupled wave-flow model in a high-energy setting: The mouth of the Columbia River. *J. Geophys. Res. Oceans* **117**, (2012).

43. Lyddon, C. E., Brown, J. M., Leonardi, N., Saulter, A. & Plater, A. J. Quantification of the Uncertainty in Coastal Storm Hazard Predictions Due to Wave-Current Interaction and Wind Forcing. *Geophys. Res. Lett.* **46**, 14576–14585 (2019).
44. Yin, K., Xu, S., Huang, W. & Xie, Y. Effects of sea level rise and typhoon intensity on storm surge and waves in Pearl River Estuary. *Ocean Eng.* **136**, 80–93 (2017).
45. Treasury, H. M. The green book: Central government guidance on appraisal and evaluation. *Lond. HM Treas.* (2018).
46. Penning-Rowsell, E. *et al. Flood and Coastal Erosion Risk Management A Manual for Economic Appraisal*. (2013).
47. Anguelov, D. *et al.* Google street view: Capturing the world at street level. *Computer* **43**, 32–38 (2010).
48. Gale, C. G., Singleton, A. D., Bates, A. G. & Longley, P. A. Creating the 2011 area classification for output areas (2011 OAC). *J. Spat. Inf. Sci.* **2016**, 1–27 (2016).
49. Day, B. & Smith, G. Outdoor Recreation Valuation (ORVal) Data Set Construction. *Rep. Dep. Food Rural Aff.* (2016).
50. Day, B. & Smith, G. S. The outdoor recreation valuation (ORVal) tool: technical report, January 2018. *Rep. Dep. Food Rural Aff. Lond.* (2017).
51. Morton, D. *et al. Final Report for LCM2015 -the new UK land cover map*. 112 (2015).
52. Symonds, A. M. *et al.* Comparison between Mike 21 FM, Delft3D and Delft3D FM flow models of western port bay, Australia. *Coast. Eng.* 2 (2016).